Journal of Proteomics 253 (2022) 104457

Contents lists available at ScienceDirect

Journal of Proteomics

journal homepage: www.elsevier.com/locate/jprot

TMT based proteomic profiling of *Sophora alopecuroides* leaves reveal flavonoid biosynthesis processes in response to salt stress

Tian-Li Ma [a,b,1,*], Wen-Juan Li [a,b,1], Yuan-Shu Hong [a,b], Yu-Mei Zhou [a,b], Lei Tian [a,b], Xiao-Gang Zhang [a,b], Feng-Lou Liu [a,b], Ping Liu [a,b,*]

[a] School of Agriculture, Ningxia University, Yinchuan, Ningxia 750021, China
[b] Key Laboratory of Modern Molecular Breeding for Dominant and Special Crops in Ningxia, Yinchuan, Ningxia 750021, China

ARTICLE INFO

Keywords:
Sophora alopecuroides
Proteomic
Salt stress
TMT
PRM

ABSTRACT

Salt stress is the major abiotic stress worldwide, adversely affecting crop yield and quality. Utilizing salt tolerance genes for the genetic breeding of crops is one of the most effective measures to withstand salinization. *Sophora alopecuroides* is a well-known saline-alkaline and drought-tolerant medicinal plant. Understanding the underlying molecular mechanism for *Sophora alopecuroides* salt tolerance is crucial to identifying the salt-tolerant genes. In this study, we performed tandem mass tag (TMT) based proteomic profiling of *S. alopecuroides* leaves under 150 mM NaCl induced salt stress condition for 3 d and 7 d. Data are available on ProteomeXchange (PXD027627). Furthermore, the proteomic findings were validated through parallel reaction monitoring (PRM). We observed that the expression levels of several transporter proteins related to the secondary messenger signaling pathway were altered under salt stress conditions induced for 3 d. However, the expression of the certain transferase, oxidoreductase, dehydrogenase, which are involved in the biosynthesis of flavonoids, alkaloids, phenylpropanoids, and amino acid metabolism, were mainly alerted after 7 d post-salt-stress induction. Several potential genes that might be involved in salt stress conditions were identified; however, it demands further investigation. Although salt stress affects the level of secondary metabolites, their correlation needs to be investigated further.

Significance: Salinization is the most severe abiotic adversity, which has had a significant negative effect on world food security over the time. Excavating salt-tolerant genes from halophytes or medicinal plants is one of the important measures to cope with salt stress. *S. alopecuroides* is a well-known medicinal plant with anti-tumor, anti-inflammatory, and antibacterial effects, anti-saline properties, and resistance to drought stress. Currently, only a few studies have explored the *S. alopecuroides*' gene function, and regulation and these studies are mostly related to the unpublished genome sequence information of *S. alopecuroides.* Recently, transcriptomics and metabolomics studies have been carried on the abiotic stress in *S. alopecuroides* roots. Multiple studies have shown that altered gene expression at the transcript level and altered metabolite levels do not correspond to the altered protein levels. In this study, TMT and PRM based proteomic analyses of *S. alopecuroides* leaves under salt stress condition induced using 150 mM NaCl for 3 d and 7 d was performed. These analyses elucidated the activation of different mechanisms in response to salt stress. A total of 434 differentially abundant proteins (DAPs) in salt stress conditions were identified and analyzed. For the first time, this study utilized proteomics technology to dig out plentiful underlying salt-tolerant genes from the medicinal plant, *S. alopecuroides*. We believe that this study will be of great significance to crop genetics and breeding.

1. Introduction

Soil salinization is widely prevalent, and it is a severe agricultural problem worldwide. It affects almost 6% of the total land and 20% of irrigated land across the globe [1–4]. Numerous crops and vegetables, such as maize, rice, and lettuce, are sensitive to salt stress [5–7]. Also, it adversely affects the yield and quality of crops, resulting in substantial economic losses. Salt stress caused a global annual economic loss of

* Corresponding author at: School of Agriculture, Ningxia University, No. 489, Helanshan West Road, Xixia District, Yinchuan, Ningxia 750021, China.
E-mail addresses: tianlima2018@163.com (T.-L. Ma), liupnxdx@126.com (P. Liu).
[1] These authors contributed equally to this work.

https://doi.org/10.1016/j.jprot.2021.104457
Received 1 August 2021; Received in revised form 26 November 2021; Accepted 9 December 2021
Available online 18 December 2021

$27.3 billion in 2014 [8]. Due to global warming and extreme weather condition, salinization, along with other environmental stress conditions, such as drought and cold, may evolve into a severe threat to global food security [2,9]. Over the years, researchers have explored various methods, such as silicon or exogenous proline, plant growth-promoting rhizobacteria (PGPR), operating seed biopriming techniques, and nanoparticles to identify salt-tolerant genes and cultivation of salt-tolerant varieties to alleviate the impact of salt stress on crops [10–15].

Sophora alopecuroides is a perennial herb that belongs to the genus *Sophora* of the Fabaceae family [16]. It is widely distributed in arid, semi-arid, and grassland areas in the west and central Asia [17–19]. Previous studies on the *S. alopecuroides* growth characteristics and other experimental evidence have shown that *S. alopecuroides* can resist salinity, alkalinity, and drought [20–22]. Besides, the application of adequate potassium supplementation and engineered nanomaterials (single-walled carbon nanohorns and ZnO nanoparticles) could improve the salt tolerance response of *S. alopecuroides* [23,24].

A total of 128 active ingredients, such as alkaloids, flavonoids, steroids, and polysaccharides, were isolated from *S. alopecuroides* [25]. These vital secondary metabolites, specifically alkaloids, make *S. alopecuroides* have anti-tumor, anti-inflammatory, antibacterial, anti-dysentery, cardioprotective, antioxidant, and antidepressant activities [20,26,27].

Currently, only the chloroplast genome of *S. alopecuroides* is available, and it contains a total of 129 genes [28]. Till now, only a few studies have explored the *S. alopecuroides'* gene function and regulation. Omics studies, such as transcriptomics, metabolomics, proteomics, ionomics, and phenomics, could elucidate the salinity and drought resistance in *S. alopecuroides*. For instance, the genetic diversity and population structure of *S. alopecuroides* were analyzed using transcriptomic SSR markers [29]. Besides, crucial gene families and biological pathways involved in major abiotic stresses (salt, alkali, and drought) were revealed through *de novo* transcriptome sequencing [22]. An integrated transcriptomics and metabolomics analysis discerned that activation of phenylpropane biosynthesis pathway involving synthesis of lignin and flavonoids might be one of the important mechanisms in *S. alopecuroides* in response to salt stress [30].

Proteins directly participate in various biological processes of plants [31–34]. Therefore, analysis of the total proteome is crucial to identifying the relevant cell signal transduction processes and regulatory mechanisms [35–38]. However, multiple studies have shown that altered gene expression at the transcript level does not correspond to the altered protein levels. The mRNA and protein levels are often asynchronous, reflecting the complexity, multidimensionality of gene expression, and regulation in plants under different stimuli [39–41]. In the current study, we performed TMT and PRM based proteomic analyses of the *S. alopecuroides* leaves, which led to the identification of deregulated genes and biological processes in response to salt stress. Besides, we also discussed the altered medicinal ingredients under salt stress conditions with an aim to excavate certain crucial salt-tolerant genes in *S. alopecuroides* under salt stress conditions.

2. Materials and methods

2.1. Plant samples and treatment

The *S. alopecuroides* seeds were collected from the teaching and experimental farm located at Ningxia University, Ningxia Hui Autonomous Region, China (106°24′ E, 38°24′ N). Seeds that were uniform in size, full, and free of insects were treated with concentrated sulfuric acid for 20 min and then rinsed with running water for 10 min. Seeds were kept in an incubator in the dark at a constant temperature of 25 °C. Once these seeds turned white, they were transplanted into flower pots with a diameter of 40 cm and cultivated in a greenhouse for 50 days. Later, the plants were irrigated with NaCl solution (gradient concentration: 0 mM, 50 mM, 100 mM, 150 mM, and 200 mM) for 3 d and 7 d. Each flowerpot was treated with 2000 mL of the corresponding concentration of NaCl by pouring the salt solution into the corresponding tray of the flowerpot. The control was the same volume of deionized water. Then, the leaves were sampled. Five seedlings were taken from each flowerpot, and three flowerpots (a total of 15 seedlings) were used as one biological replicate. At last, all leaves were mixed thoroughly and put into a tube; each tube contained 1 g of leaves, and these tubes were stored in liquid nitrogen at −80 °C for transcriptome, proteome, and other related analyses. The experiment included three groups: Z (control), F (3 d), and T (7 d). Each group contained three replicates.

2.2. Detection method of physiological indicators

The leaf chlorophyll content and SOD, POD, and CAD activities were determined spectrophotometrically. The leaf chlorophyll content was determined by measuring the absorbance at 665 nm and 649 nm. SOD activity was determined by measuring the absorbance at 560 nm using the nitroblue tetrazolium (NBT) method. Besides, the POD activity was determined by gaging the absorbance at 470 nm using guaiacol and H_2O_2 as substrate, and CAT activity was determined by measuring the absorbance at 240 nm using H_2O_2 as substrate. Proline content was determined using the acid ninhydrin method and malondialdehyde content through thiobarbituric acid reactive substance (TBARS) assay. The contents of matrine, oxymatrine, sophocarpine, and oxysophocarpine in leave samples from plants under salt stress conditions were determined using Agilent 1260 infinity II high-performance liquid chromatography (HPLC). Standard products of matrine (batch number: 110805–201709), oxymatrine (batch number: 110780–201508), oxysophocarpine (batch number: 111652–200301), and sophocarpine (batch number: 112052–202001) were purchased from the China National Institutes for Food and Drug Control, China. The Na^+ and K^+ contents in sample ashes were determined by Hitachi Z-2000 flame atomic absorption spectrometry. 火焰原子吸收法

2.3. Transcriptome sequencing and assembly

Illumina HiSeq platform was used for RNA-seq. Fastp software was used to filter raw sequencing data to clean reads. Trinity software [42] was used to splice clean reads into transcripts. These transcript sequences were later subjected to CDS prediction and function annotation analyses. Five databases, *i.e.*, Nr, Pfam, Swiss-prot, KEGG, and GO were used for gene function annotations. The original sequencing data of transcriptomics were uploaded to the SRA database in NCBI. The BioProject accession number is PRJNA748576.

2.4. Protein extraction and trypsin digestion

S. alopecuroides leaves samples were ground to a fine powder using liquid nitrogen. Protein was extracted using 4% (*w/v*) SDS in 100 mM Tris HCl (pH 7.6, 0.1 M DTT). Around 20 μg of protein from each sample was used for protein quantification using the BCA method. 200 μg of protein was taken from each sample and digested using the filter aided proteome preparation (FASP) method for trypsin digestion.

2.5. Protein TMT labeling, HPLC fractionation, and LC-MS/MS analysis

100 μg of trypsin digested protein was taken from each sample and labeled with TMT (Thermo Fisher Scientific), according to the manufacturer's instructions. Peptides from each group were pooled together and graded using high pH reversed-phase peptide fractionation kit. Each converted peptide sample was vacuum dried, lyophilized, and later resolubilized in 12 μL of 0.1% FA, and the peptide concentration was determined using a spectrometer at OD280.

Furthermore, each fractionated sample was separated using the HPLC liquid system Easy nLC with a nanoliter flow rate using buffer A (0.1% formic acid aqueous solution) and buffer B (0.1% formic acid in

84% acetonitrile aqueous solution). The chromatographic column was equilibrated with 95% of buffer A. The samples were loaded into the loading column using an autosampler (Thermo Scientific Acclaim PepMap100, 100 μm × 2 cm, nano Viper C18) and passed through the analytical column (Thermo scientific EASY column, 10 cm, ID75 μm, 3 μm, C18-A2) separation with the flow rate of 300 nL/min. These samples were analyzed on a Q-Exactive mass spectrometer. The detection method was positive ion, and the scan range for precursor ion was 300–1800 *m/z*. Resolution of the primary mass spectrometer was 70,000 at 200 m/z, AGC (Automatic gain control) target was 1e6, maximum IT was 50 ms, and the dynamic exclusion time was 60.0 s. To determine the *m/z* ratio of peptides and peptide fragments, 20 fragmentation maps were collected after each scan. The MS2 activation type was HCD, and the isolation window was 2 *m/z*. The resolution of the secondary mass spectrum was 17,500 at 200 m/z (TMT 6-plex) or 35,000 at 200 m/z (TMT 10-plex) with 30 eV normalized collision energy and 0.1% underfill. All the above were done by Shanghai Applied Protein Technology Co. Ltd. The mass spectrometry proteomics data have been deposited to the ProteomeXchange Consortium with the dataset identifier: PXD027627.

2.6. Protein identification and quantification

Mascot version 2.2 and Proteome Discoverer version 1.4 were used for analyzing MS/MS data. *S. alopecuroides* leaves RNA-seq data from our laboratory was used for protein identification using MS/MS data. Trypsin was selected as a random cleavage enzyme, and the parameter of max missed cleavages was set to 2. Carbamidomethyl (C), TMT 6/10plex (N-term), and TMT6/10 plex (K) was selected as fixed modifications. The variable modifications were set as oxidation (M), TMT 6/10plex (Y). The peptide mass tolerance was set to ±20 ppm, and the fragment mass tolerance was 0.1 Da. The database schema was used as a decoy to calculate FDR. The screening criteria for credible peptides was FDR ≤0.01. The protein ratios were calculated from the median of unique peptides only. Then, normalized all peptide ratios using the median protein ratio. The median protein ratio was 1 after the protein normalization. Plant-mPLoc software was used to predict the subcellular location of the identified proteins.

2.7. Bioinformatics analysis

A fold-change cut-off of ≥1.2 fold-change (up-regulation greater than 1.2 times or down-regulation less than 0.83 times) was used to identify differentially abundant proteins (DAP) with *P-value* < 0.05. The normalized differential proteins were subjected to cluster analysis using the R package version 3.4. Blast2Go (https://www.blast2go.com/) and KEGG Automatic Annotation Server (KAAS) were used for GO annotation and KEGG pathway analysis of target proteins. GO annotation and KEGG pathway enrichment analysis were performed using Fisher's exact test. CytoScape software was used in protein-protein interaction (PPI) analysis.

2.8. Validation of candidate proteins

The parallel reaction monitoring (PRM) technology was used to validate the expression level of 12 differential proteins identified using the proteomics analysis. Xcalibur software was used for PRM. Around 1 μg of peptides was taken from each sample, and 20 fmol of standard peptides (PRTC: ELGQSGVDTYLQTK) was used for PRM based validation. For PRM, samples fractionated using HPLC were analyzed using a Q-Exactive HF mass spectrometer (Thermo Scientific). The detection mode was positive ions. Scan range of primary mass spectrum ranged from 300 to 1800 *m/z*. The mass spectrum resolution rate was 60,000 at 200 *m/z*. The AGC target was 3e6, and the maximum IT was 200 ms. After each full MS scan, 20 PRM scans (MS2 scans) were collected based on the inclusion list. The isolation window was 1.6 Th, and the MS resolution was 30,000 at 200 m/z. The AGC target was 3e6, and the maximum IT was 120 ms. The MS2 activation type was HCD, and the normalized collision energy was 27. Skyline version 3.5.0 was used to analyze the data of the original PRM files. The criterion of quantitative analysis was selected to 3 product-ions with higher peptide abundance and as continuous as possible. The peak area of the heavy isotope-labeled internal standard peptide was corrected to obtain the relative expression information of each peptide in different samples. The average relative expression of the target peptide in each of the samples was calculated and analyzed using the *t*-test method.

In addition, we selected eight DAPs and used the Analyticyena qTOWER3G fluorescent quantitative PCR instrument to detect gene expression. The online primer design tool, Primer-Blast, was used to design primers. All primers were synthesized by Shanghai Shenggong Biological Engineering Co., Ltd. The qRT-PCR primer sequences are given in Table S1.

3. Results

3.1. Photosynthesis performances and physiological indicators in leaves of *S. alopecuroides* under salt stress condition

As per a previous study, salt-stress induced using 1.2% NaCl (≈205 mM NaCl) inhibited the growth of 4-week-old *S. alopecuroides* seedlings [22,30]. We quantified chlorophyll *a* and chlorophyll *b* levels and analyzed their ratio post 3 d and 7 d of salt stress induction to investigate the altered proteome of *S. alopecuroides* leaves in 7-week-old *S. alopecuroides* seedlings under the NaCl induced stress. The outcomes of this analysis demonstrated an apparent decrease in chlorophyll *a* and b content and their ratio under 150 mM NaCl induced salt stress for 3 d (Figures 1A and 1B). We did not observe apparent differences in leaf wilting and slow-growth phenotypes during the experimental periods (Fig. S1). Enzyme activities of superoxide dismutase (SOD), peroxidase (POD), and catalase (CAT) in *S. alopecuroides* leave under 150 mM NaCl induced salt stress for 3 d, and 7 d was estimated. The contents of malondialdehyde (MDA), proline, Na^+, K^+, and the ratio of K^+/Na^+ in *S. alopecuroides* leaves were quantified under the same salt stress condition. The results showed that dynamic changes of the SOD, POD, and CAT activities in response to salt stress were different. The activity of SOD increased when *S. alopecuroides* seedlings were subjected to salt stress for 7 d. Besides, the activity of POD and CAT increased when *S. alopecuroides* seedlings were subjected to salt stress for 3 d, but it decreased under salt stress for 7 d. In addition, the MDA, proline, and Na^+ levels increased gradually, while the K^+ levels and K^+/Na^+ ratio decreased gradually under salt stress conditions for 3 d to 7 d (Figure 1C).

3.2. Protein identification

The TMT-based quantitative proteomic analysis was performed to analyze the dynamic change of proteins in the control (Z group) and salt stress condition induced using 150 mM NaCl for 3 d (F group) and 7 d (T group). A total of 400,515 spectra were obtained, of which 70,693 were the matched peptide spectrums. Total 25,192 and 21,269 unique peptides were obtained, respectively. We identified a total of 5505 proteins (IPs) (Table 1).

PCA plots analysis of the IPs showed that three biological replicates per group had good repeatability, indicating the high quality of data for effective statistical analysis (Figure 2A). We observed diverse subcellular localization of IPs. Out of total IPs, 29%, 24%, and 11% IPs were located in the cytoplasm, nucleus, and plasma membrane, respectively. Other IPs were either localized at chloroplast, mitochondria or were extracellular (Figure 2B).

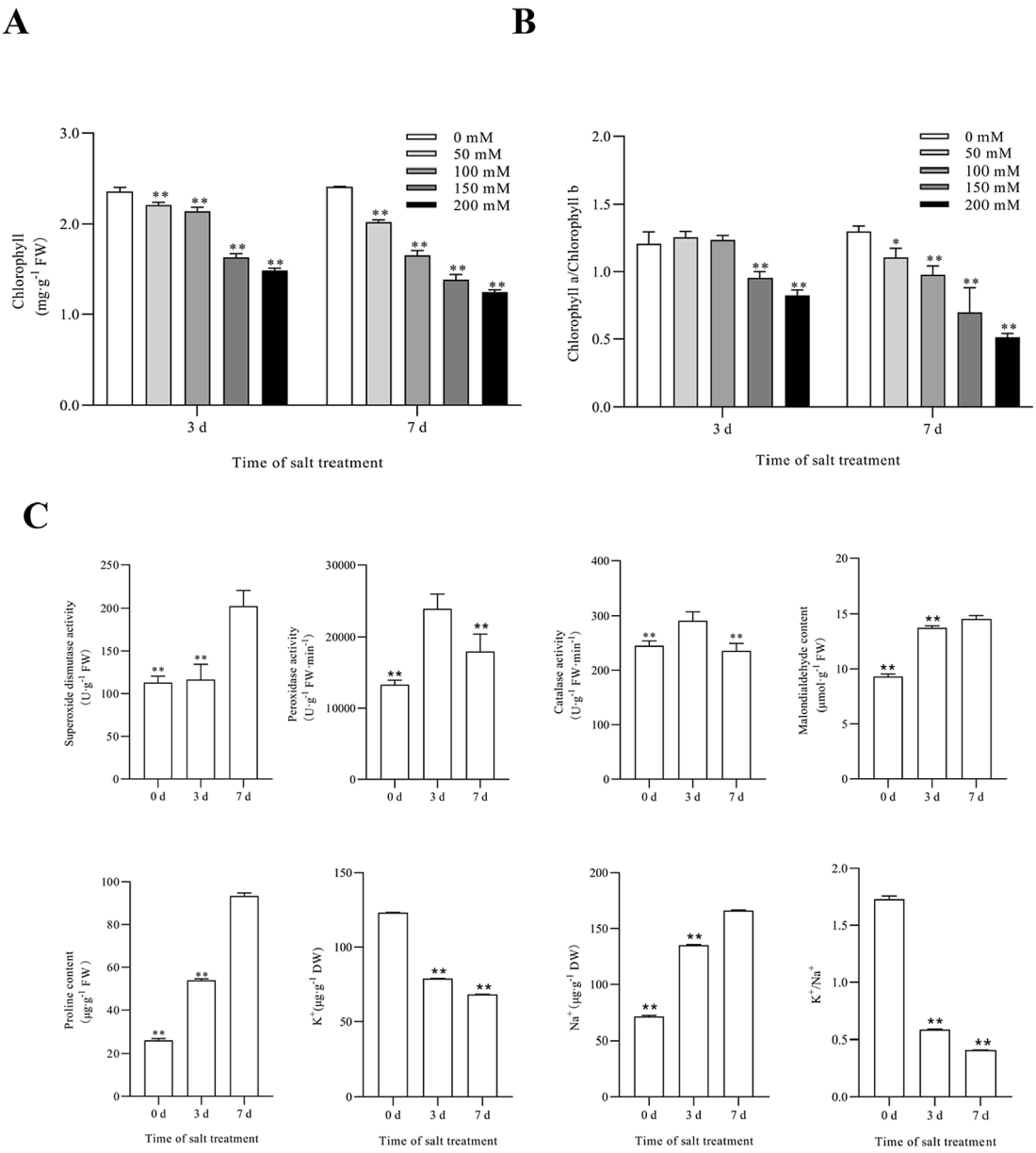

Fig. 1. Determination of physiological indices of *S. alopecuroides* leaves under salt stress conditions. (A) Comparison of the chlorophyll levels in leaves under salt-stress conditions induced using different NaCl concentrations. (B) Comparison of the chlorophyll *a*/chlorophyll *b* ratio in leaves under salt-stress conditions induced using different NaCl concentrations. (C) Determination of SOD, POD, CAT, MDA, proline, Na^+ and K^+ content, and K^+/Na^+ ratio under 150 mM NaCl induced salt stress condition. The vertical bar represents the mean + SD calculated from three replicates. Each variable was statistically used Fisher's Least Significant Difference (LSD) test compared with the control (**$P < 0.01$, *$P < 0.05$).

Table 1
Summary of identified proteins.

Name	Information
Database	Self-built transcriptomics database
Total Spectrums	400,515
Matched Peptide Spectrums	70,693
Peptides	25,192
Unique peptides	21,269
Identified proteins	5505
Quantifiable proteins	5466

3.3. Quality control of MS data

High quality of MS data is the first step to obtaining credible proteomics results. The outcomes of the proteomic analysis showed that the ion score for 78.41% peptides exceeded 20 with 33.55 median score based on the Peptide IonScore Distribution (Figure 3A). In addition, the mass error of the majority of peptides ranged from −10 ppm to 10 ppm. This indicated the high mass accuracy of MS data (Figure 3B). > 95% of the peptides were 5 to 23 amino acid residues long (Figure 3C). Besides, the number of peptides corresponding to almost 70% of the identified proteins was ≥2, which indicated that the MS data could be further analyzed (Figure 3D). The detailed information of identified protein is shown in Table S2.

3.4. Transcriptomics sequencing, assembly, and functional annotation of genes

S. alopecuroides gene annotation was not available when the current study was conducted. The first article on "no-reference transcriptome

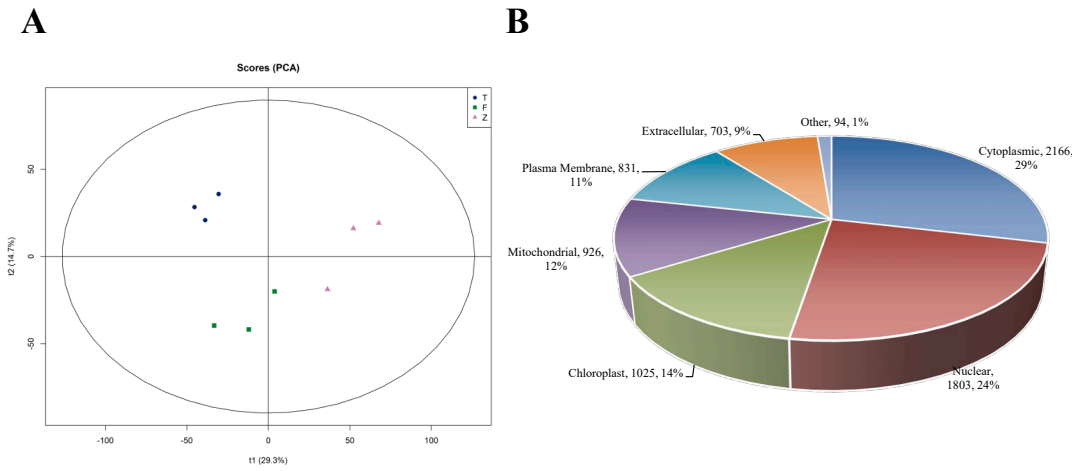

Fig. 2. Overview of a time course of *S. alopecuroides* response to salt stress. (A) PCA plots of proteins identified in Z, F, and T groups. (B) The distribution of the subcellular locations of proteins identified in Z, F, and T groups.

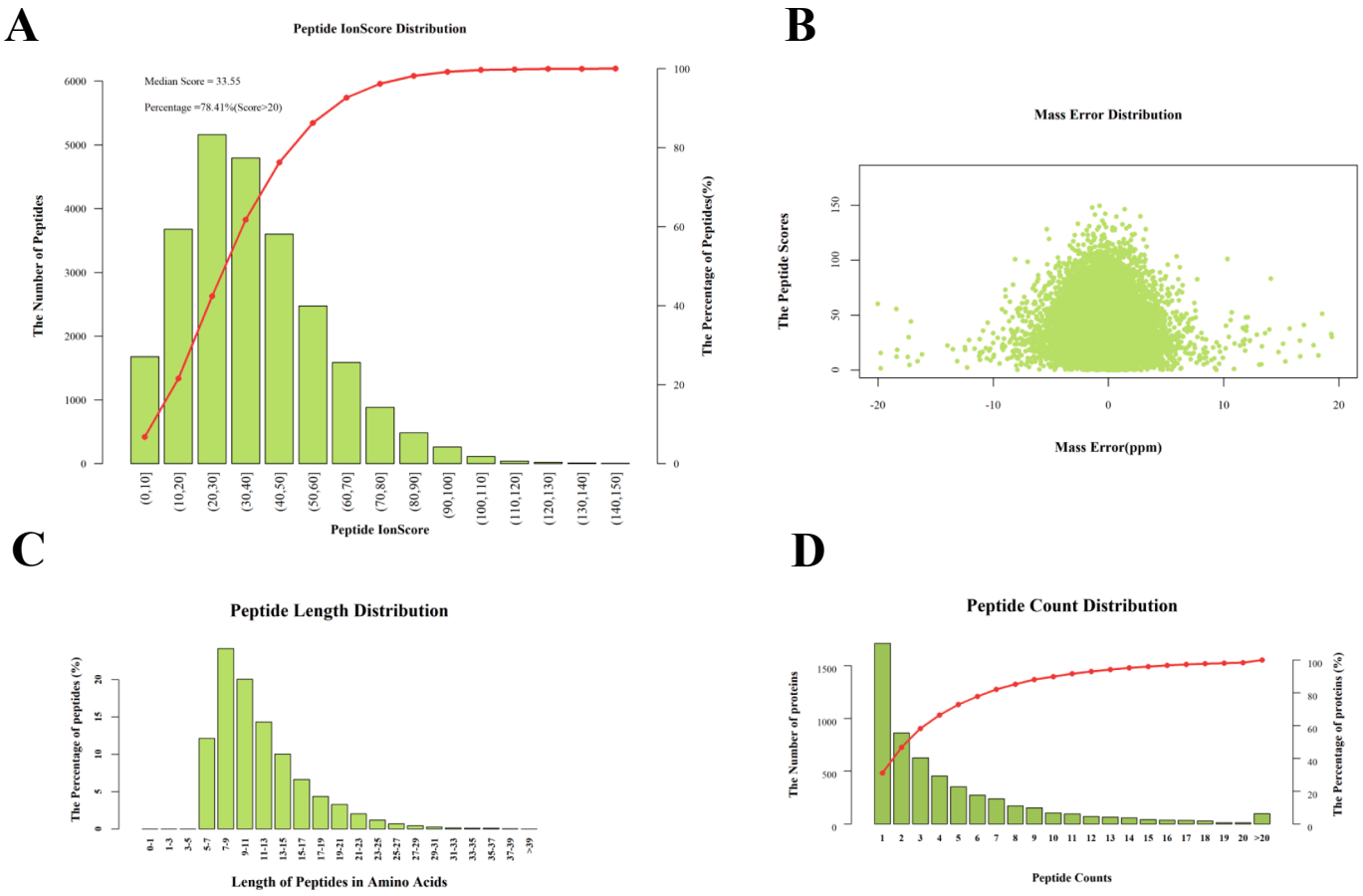

Fig. 3. The critical quality control of MS data. (A) The peptide ion score distribution of IPs. (B) The mass error of distribution of IPs. (C) The peptides length distribution of IPs. (D) The peptides count distribution of IPs.

sequencing" in *S. alopecuroides* under stress conditions was published in 2020, wherein differentially expressed genes (DEGs) under salt, alkali, and drought stress conditions in *S. alopecuroides* were analyzed [22]. Thus, firstly we performed *de novo* transcriptomic sequencing of *S. alopecuroides* leaves under the 150 mM NaCl induced salt stress condition for 0 d (Z group), 3 d (F group), and 7 d (T group). These experimental conditions were identical to that of the proteomics experiment. In total, 424,809,870 raw reads and 420,832,634 clean reads were obtained from the 3 groups and 9 samples (Table 2). 58.18 Gb of clean bases were obtained. The Q20 of almost all samples was above 97%, indicating the high accuracy of transcriptome sequencing (Table 2).

A total of 661,814 transcripts and 415,804 unigenes, with an average length of 749 bp and 539 bp, respectively, were obtained. Out of these transcripts, 50% unigenes (235,279) were $\leq$ 300 bp long, and about 76% unigenes (316,422) were $\leq$ 500 bp long. Around 11.4% unigenes (47,326) were $\geq$ 1000 bp long (Fig. S2). Nr database was compared and annotated, and we observed that several species had high gene sequence

Table 2
Analysis of RNA-seq results for each sample.

Sample	Raw_reads	Clean_reads	Clean_bases	Error(%)	Q20(%)	Q30(%)	GC(%)
Z1	55,099,296	54,570,770	7.6 G	0.03	97.35	92.47	44.89
Z2	42,195,994	41,687,964	5.72 G	0.03	97.12	92.01	46.8
Z3	42,995,490	42,671,428	5.89 G	0.03	97.58	92.88	46.63
F1	47,284,546	46,902,492	6.49 G	0.03	97.44	92.71	49.67
F2	56,265,728	55,691,110	7.66 G	0.03	97.32	92.42	45.95
F3	43,083,560	42,761,810	5.93 G	0.03	97.68	93.22	46.52
T1	45,979,276	45,544,448	6.29 G	0.03	97.6	93.02	47.45
T2	48,486,388	48,076,938	6.66 G	0.03	97.4	92.56	45.53
T3	43,419,592	42,925,674	5.94 G	0.03	96.88	91.38	44.08
Summary	424,809,870	420,832,634	58.18 G				

Q20: percentage of bases with a Phred value >20
Q30: percentage of bases with a Phred value >30.

similarity with *S. alopecuroides,* such as *Lupinus angustifolius*, *Cajanus cajan*, and *Ricinus communis* (Fig. S3).

To obtain comprehensive gene function information and study the function of these genes, we performed gene function annotations of five major databases: NR, PFAM, Swiss-Prot, KEGG, and GO. The highest number of genes, *i.e.*, 140,678 (33.83%), were annotated in the NR (NCBI redundant protein Sequences) database, followed by 76,501 (18.4%) genes in the Swiss-Prot database, 63,868 (15.36%) in the PFAM database, 62,905 (15.13) in the GO database, and 21,537 (5.18%) in the KO database (Table 3). Thus, the number of genes successfully annotated in at least one of the above five databases was 153,893 (37.01%).

3.5. Identification and analysis of differentially abundant proteins

Fold-change cut-off of $\geq$1.2 and $P < 0.05$ for up-regulated proteins and $\leq$ 0.83 and $P < 0.05$ for down-regulated proteins was applied to identify the differentially abundant proteins (DAPs) between F *vs.* Z, T *vs.* Z, and T *vs.* F. A total of 434 DAPs were identified under salt stress conditions compared to control. Hierarchical cluster analysis showed six apparent clusters at two time points (salt stress for 3 d and 7 d) and good repeatability between different samples of the same group (Figure 4A). We observed four different expression trends in six clusters. The protein expression of cluster 1 and cluster 3 continued to decrease from 3 d to 7 d post-salt-stress induction, while cluster 4 showed the opposite trend. With increasing stress levels, the protein expression of cluster 6 first decreased and then increased; contrastingly, the protein expression of cluster 2 and cluster 5 first increased and then decreased (Figure 4B). In F *vs.* Z, 61 DAPs were up-regulated, and 66 DAPs were down-regulated, whereas in T *vs.* Z, 135 DAPs were up-regulated, and 112 DAPs were down-regulated. This indicated that NaCl treatment time was directly correlated to DAPs in response to salt stress. In T *vs.* F, 37 DAPs were up-regulated, and 23 DAPs were down-regulated (Figure 4C).

A Venn diagram analysis was performed to identify the common and DAPs participating in the early to mid-stage salt stress. In this analysis, up-regulated and down-regulated genes between F *vs.* Z, T *vs.* Z, and T *vs.* F were used as input. As per the Venn diagram analysis, three common up-regulated genes and no common down-regulated genes were observed between the three groups (Figure 4D). These three DAPs were subjected to in-depth analysis. Besides, 18 DAPs were up-regulated, and 9 DAPs were down-regulated between T *vs.* F and T *vs.* Z groups, 29 DAPs were up-regulated, and 37 DAPs were down-regulated between F *vs.* Z and T *vs.* Z groups, and 3 DAPs were up-regulated and 0 DAPs were down-regulated between T *vs.* F and F *vs.* Z (Figure 4D).

Table 3
Overview of gene function annotations in different databases.

Type	Number of Unigenes	Percentage (%)
Annotated in NR	140,678	33.83
Annotated in SwissProt	76,501	18.4
Annotated in PFAM	63,868	15.36
Annotated in GO	62,905	15.13
Annotated in KO	21,537	5.18
Annotated in all Databases	9948	2.39
Annotated in at least one Database	153,893	37.01
Total Unigenes	415,804	100

3.6. GO enrichment analysis of DAPs

In the GO enrichment analysis of DAPs from the F *vs.* Z group, DAPs were significantly enriched into 103 functional GO terms, of which 43 belonged to biological processes (BPs), 57 to molecular functions (MFs), and 3 to cellular components (CCs) (Table S3). The top 20 enriched GOs were obtained using the Fisher's Exact Test (Figure 5A). Cell wall biogenesis, monosaccharide transmembrane transport, hexose transmembrane transport, glucose transmembrane transport, and glucose import were the most significantly enriched GOs in the BP category. The transporter activity, secondary active transmembrane transporter activity, beta-galactosidase activity, transmembrane transporter activity, ion transmembrane transporter activity, galactosidase activity, and other transporter's activities were the most significantly enriched GOs terms in the MF category. Besides, the most significant GOs terms enriched in the CC category were related to the membrane, including the integral component of the membrane and the intrinsic component of the membrane.

GO enrichment analysis of DAPs identified from T *vs.* Z group resulted in enrichment of 106 functional GO terms, of which 42 belonged to BPs, 49 to MFs, and 15 to CCs (Table S4). The top 20 GOs were obtained using the Fisher's Exact Test (Figure 5B). The cell wall organization or biogenesis, transition metal ion transport, flavonoid metabolic process, external encapsulating structure organization, cell wall organization, and iron ion transport were the most significantly enriched GO terms in the BP category. The beta-galactosidase activity, oxidoreductase activity (oxidizing metal ions, oxygen as acceptor), protochlorophyllide reductase activity, ferroxidase activity, ferric iron binding, galactosidase activity, glucosyltransferase activity, and structural constituent of cytoskeleton were the most significantly enriched GO terms in the MF category. The most significantly enriched GOs terms in the CC category were external encapsulating structure, cell wall, supramolecular complex, and so on.

GO enrichment analysis of DAPs identified from T *vs.* F group resulted in enrichment of 37 functional GO terms, of which 13 belonged to BPs, 12 to MFs, and 12 to CCs (Table S5). The top 20 GOs were obtained from the Fisher's Exact Test (Figure 5C). The mitochondrial respiratory chain complex assembly, NADH dehydrogenase complex assembly, oxazole or thiazole metabolic process, oxazole or thiazole biosynthetic process, and microtubule-based process were the most significantly enriched GO terms in the BP category. The protochlorophyllide reductase activity, structural constituent of the cytoskeleton, transferase activity (transferring alkyl or aryl, other than methyl groups), oxidoreductase activities (CH-CH group of donors, NAD or NADP as acceptor) were the most significantly enriched GO terms in

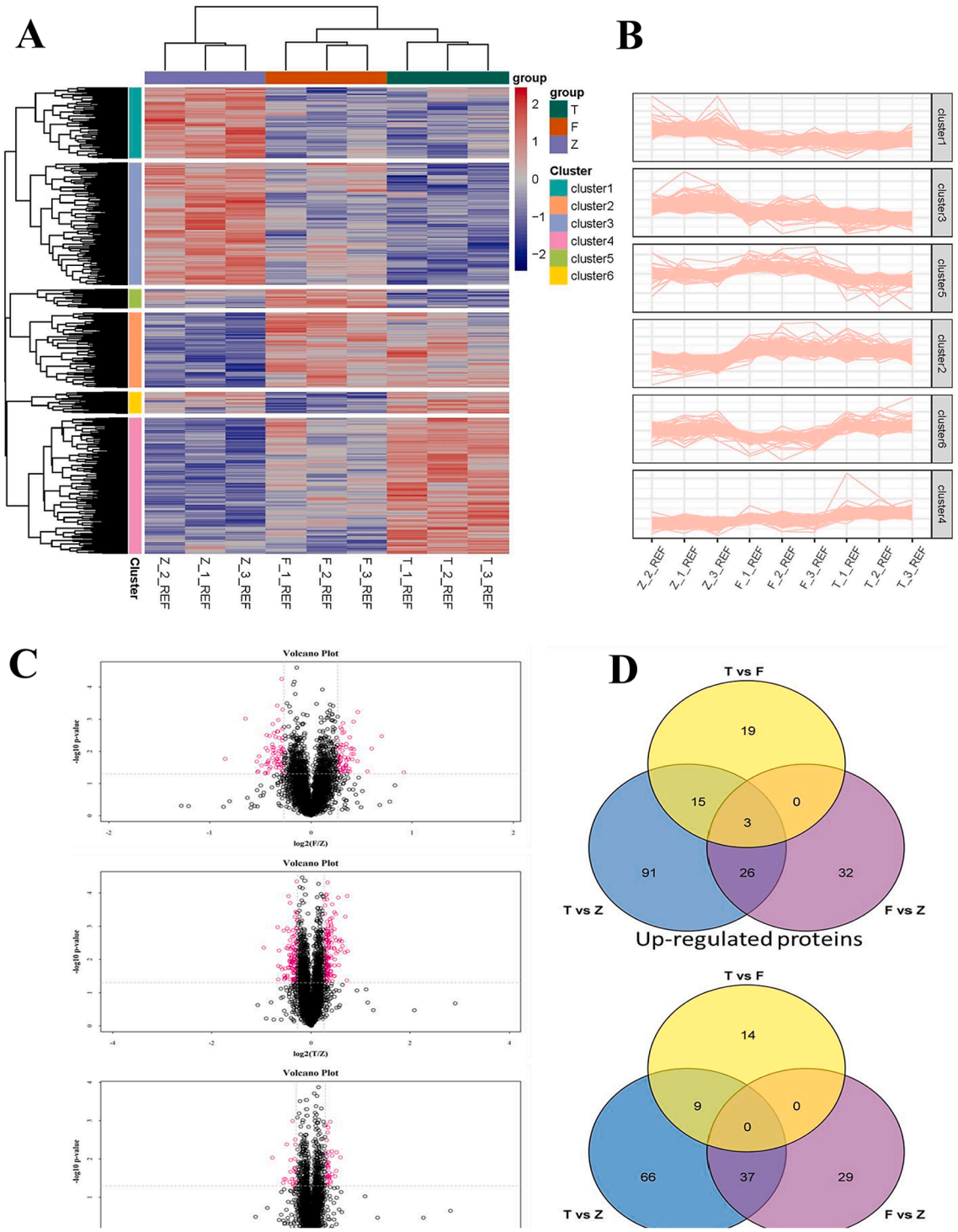

Fig. 4. Analysis of differentially abundant proteins (DAPs) in all compared groups. (A) Hierarchical cluster analysis of all DAPs. (B) The line graph of different expression trends in six clusters. (C) The volcano plots of DAPs in F *vs.* Z, T *vs.* Z, and T *vs.* F. (D) Venn diagram of up-regulated and down-regulated DAPs in the F *vs.* Z, T *vs.* Z, and T *vs.* F.

the MF category. The most significant GO terms enriched in the CC category were transcription factor TFIID complex, supramolecular complex, supramolecular polymer, and so on.

3.7. KEGG pathway enrichment analysis of DAPs

KEGG pathway analysis is one of the most systematic and comprehensive methods to understand the activation of the physiological and biochemical processes under stress conditions. DAPs from different groups were subjected to KEGG analysis. KEGG enrichment analysis of DAPs from the F *vs.* Z group showed enrichment of 96 pathways. Some of these enriched pathways were the phosphatidylinositol signaling system, cAMP signaling pathway, calcium signaling pathway, plant-pathogen interaction, MAPK signaling pathway in plants, and porphyrin and chlorophyll metabolism (Table S6). It is worth noting that most of the significantly enriched KEGG pathways were related to crucial animal signaling pathways except the cAMP signaling pathway and phosphatidylinositol signaling system (Figure 6A).

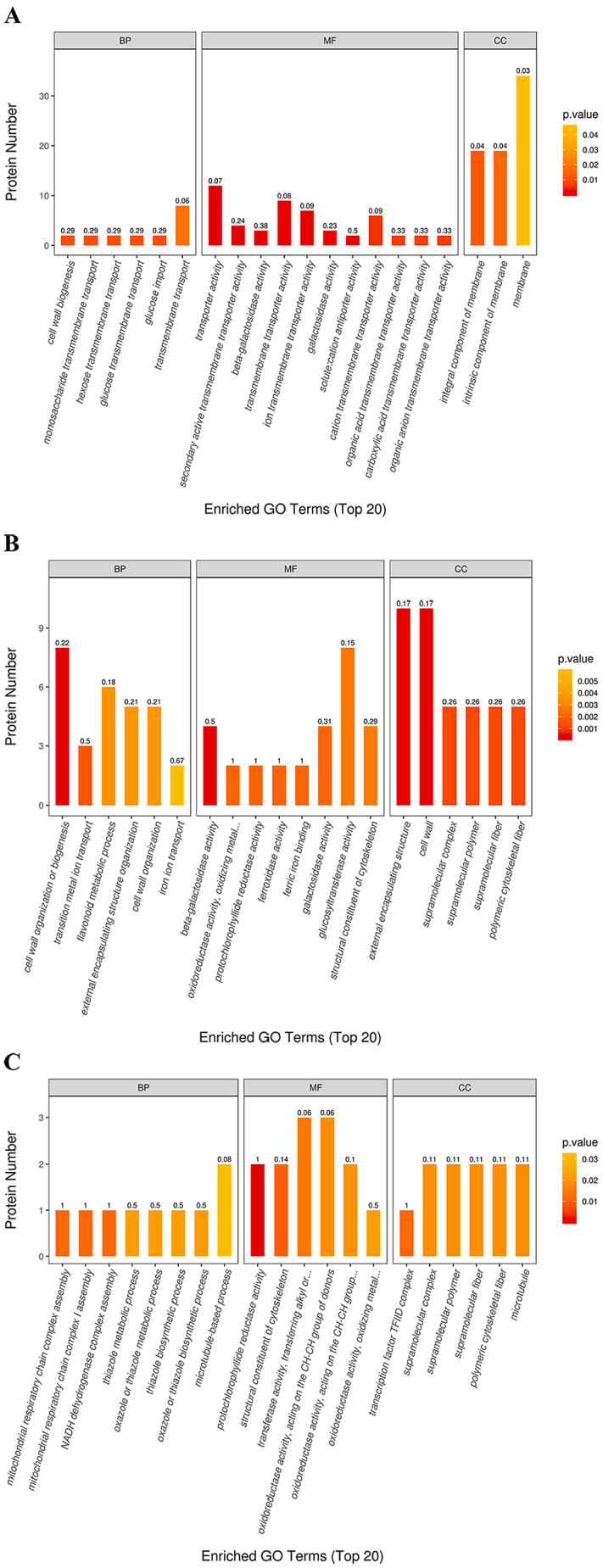

Fig. 5. Gene Ontology (GO) analysis of DAPs from different groups. The significantly enriched top 20 GO terms in (A) F group *vs.* Z group, (B) T group *vs.* Z group, and (C) T group *vs.* F group.
The color gradient represents *P*-value below 0.05. The darker the color (closer to red), the smaller the *P-value* and higher the significance of the enriched GOs. The number above the bar graph represents the enrichment factor (richFator $\leq$1). It represents the ratio of the number of DAPs annotated to a GO functional category to the number of all identified proteins annotated to the GO functional category. BP, biological process; MF, molecular function; CC, cellular component. (For interpretation of the references to color in this figure legend, the reader is referred to the web version of this article.)

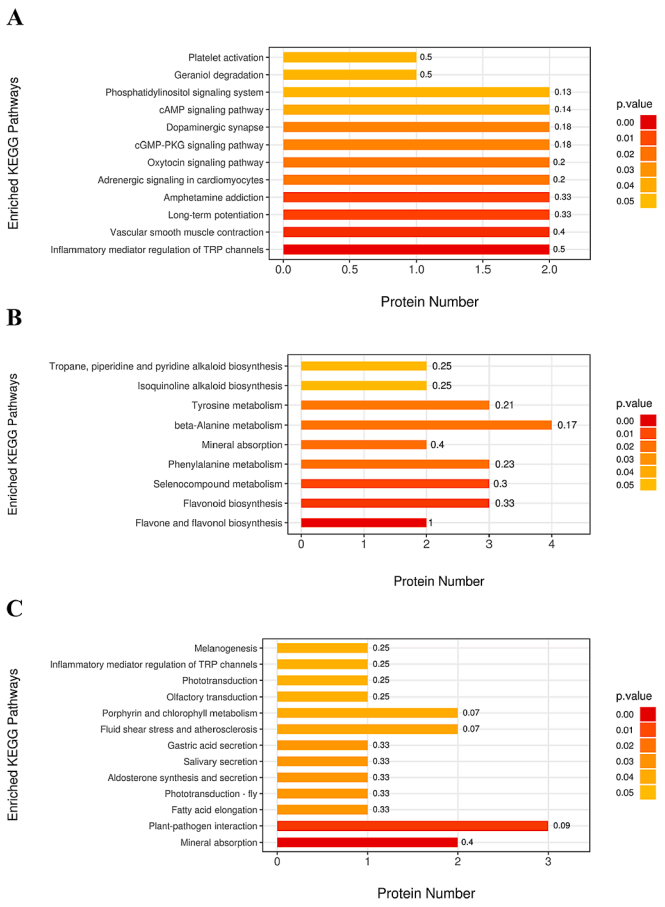

Fig. 6. KEGG pathway enrichment analysis of DAPs from different groups. The significantly enriched KEGG pathways in DAPs from (A) F group *vs.* Z group, (B) T group *vs.* Z group, and (C) T group *vs.* F group.
The color gradient represents the *P*-value below 0.05. The darker the color (closer to red), the smaller the *P*-value, and the more significant is the enriched KEGG pathways. The number above the bar graph represents the enrichment factor (richFator ≤1). It indicates the ratio of the number of DAPs annotated to a KEGG pathway to the number of all identified proteins annotated to the KEGG pathways. (For interpretation of the references to color in this figure legend, the reader is referred to the web version of this article.)

A total of 92 pathways were enriched in the KEGG pathway enrichment analysis of DAPs from T *vs.* Z group (Table S7). The significantly enriched KEGG pathways could be divided into three categories: a) flavone, flavonol, and flavonoid biosynthesis, b) amino acid metabolisms, such as phenylalanine, beta-alanine, and tyrosine metabolisms; and c) alkaloid biosyntheses, such as isoquinoline alkaloid, tropane, piperidine, and pyridine alkaloid biosynthesis (Figure 6B). In KEGG pathway enrichment analysis of DAPs between the T *vs.* F group, a total of 73 pathways were enriched (Table S8), of which 13 were significantly enriched, which were mainly related to mineral absorption and plant-pathogen interaction (Figure 6C).

3.8. PRM and RT-qPCR based validation of TMT data

To validate the TMT data, 32 and 8 proteins were randomly selected for parallel reaction monitoring (PRM) and RT-qPCR, respectively. We found that 12 proteins could be quantitative monitor reliable peptides out of the total 32 target proteins used for PRM analysis. Out of these 12 proteins, the expression of 9 proteins was highly consistent between TMT and PRM analysis (Figure 7A).

For the RT-qPCR-based validation study, six candidate proteins were divided into two categories based on their function: a) signal transduction proteins, including calmodulin, calcium-binding proteins, and serine/threonine-protein phosphatase PP1 catalytic subunit and b) plant secondary metabolites. For instance, chalcone synthase and flavonol-3-*O*-glucoside L-rhamnosyl transferase were referred to as flavonoid biosynthesis. Primary-amine oxidase was related to isoquinoline alkaloid biosynthesis. 4-hydroxyphenylpyruvate dioxygenase and methionine-gamma-lyase were relevant to amino acid metabolism. The results showed that the mRNA expression of six related genes was either up-regulated or down-regulated according to the T *vs.* Z group (Figure 7B).

4. Discussion

4.1. Comparison of different omics studies on S. alopecuroides under salt stress condition

The outcomes of this study showed similarities as well as differences from previous studies. Firstly, the omics techniques applied to the salt tolerance mechanism in *S. alopecuroides* were different. In the previous studies by Yan's [22] and Zhu's, transcriptomics and integrated transcriptomic and metabolomic techniques were used, respectively [30], while the current study employed proteomics. Secondly, experimental designs in the current and previous studies are different. In the study by Yan and Zhu, experimental components (salt stress condition: 200 mM NaCl, seedling age: four-week-old *S. alopecuroides*; treatment time-points: 0 h, 4 h, 24 h, 48 h, and 72 h, and tissue: roots) were different from the current study (salt stress condition: 150 mM NaCl, seedling age: seven-week-old *S. alopecuroides*; treatment time-points: 0 h, 3 d, and 7 d, and tissue: leaves). Yan and Zhu's study found the obvious stress phenotypes of *S. alopecuroides* under salt stress condition induced using 200 mM NaCl induced for 72 h. However, in the current study, apparent differences in leaf wilting and slow-growth phenotypes under the salt stress condition induced using 150 mM NaCl for 3 d and 7 d were not observed. It might be caused by the differences in seedling age and relatively low NaCl concentration. Seven-week-old seedlings were more salt-tolerant than four-week-old seedlings. Thirdly, the research conclusions were not completely consistent. Yan et al. identified 1673 differentially expressed genes, and the number of down-regulated genes (1519) was more than the number of up-regulated genes (159). The results revealed differential expression of crucial candidate genes in response to salt stress, including certain transcription factors, such as *SaMYB1*, *SaMYB5*, *SaMYB14*, *SabZIP3*, and *SabZIP5*. In the current study, a total of 434 DAPs from salt stress conditions were identified and analyzed, but transcription factors involved in salt stress were less. It indicated that altered gene expression was at the transcript level, and altered levels of metabolites do not correspond to the altered protein levels in *S. alopecuroides*. However, there were some similarities in the experimental results. Zhu et al. elucidated the key role of the phenylpropanoid biosynthesis pathway, the lignin and flavonoid synthesis pathways in response to salt stress in the roots of *S. alopecuroides*. In the current study, differential expression of proteins involved in the biosynthesis of flavonoids, alkaloids, phenylpropanoids, and amino acid metabolism was identified. From the above analysis, we can conclude that no matter what kind of tissues and omics technologies were adopted, phenylpropane metabolism was always the vital response pathway to *S. alopecuroides* under salt stress. The phenylpropane pathway is recognized to be the most comprehensively studied secondary metabolic pathway in plants, producing more than 8000 metabolites, such as flavonoids, phenols, lignin, lignans, tannins, *etc.* [43]. A broad of studies have found that the phenylpropane pathway can be activated under abiotic and biotic stresses [43,44]. It is worth noting that some members of the MYB transcription factor positively participate in the phenylpropane pathway under various stresses [43]. However, the types and concentrations of the main phenylpropanoid metabolites produced by different plant species under salt stress conditions are inconsistent, which may be caused by dissimilar molecular genetic mechanisms [44].

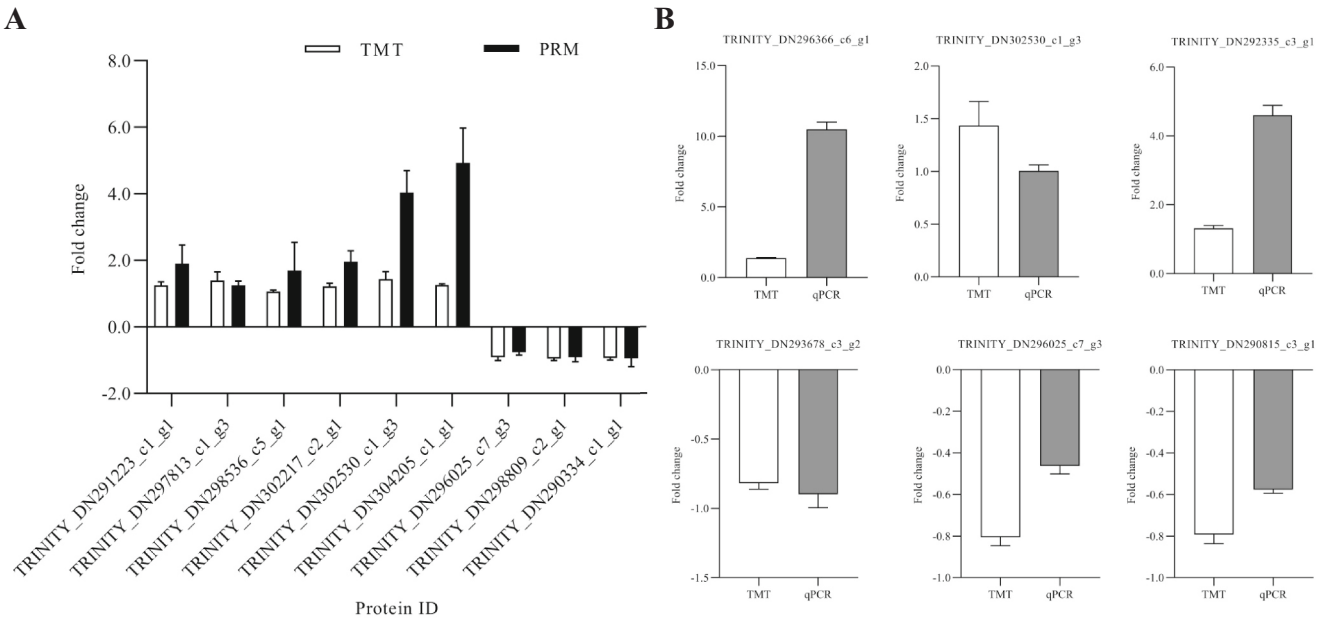

Fig. 7. Validation of TMT data through PRM and qRT-PCR based analysis. (A) Comparison of the relative expression levels of selected proteins identified using TMT and PRM. (B) qRT-PCR based analysis of DAPs from control *vs.* salt-treated (7 d) group of *S. alopecuroides*leaves. Each analysis included three biological replicates.

Our project found that the expression of flavonoid branch-related proteins in the phenylpropane pathway of *S. alopecuroides* under salt stress has changed extensively. Determining the content of flavonoids metabolites will be beneficial to further understand the salt resistance mechanism of *S. alopecuroides*. Although our results found that the content of some alkaloids increased under salt stress, the expression of the alkaloids pathway-related proteins has not changed significantly. It is probable because the proteins related to alkaloid synthesis are regulated and modified at the transcription level, post-transcriptional level, or post-translational level in *S. alopecuroides* under salt conditions.

No apparent physiological phenotypes such as plant growth inhibition, leaf wilting, and yellowing leaves were observed in the seven-week-old *S. alopecuroides* seedlings under salt stress conditions induced using 150 mM NaCl stress for 3 d; however, we observed significantly reduced chlorophyll content at this stage. Compared with the earlier stage (0, 4, 24, 48 h) of salt stress, the chlorophyll content firstly decreased and then increased from 4 h to 24 h, MDA level increased from 4 h to 48 h through self-regulation of *S.* alopecuroides [30]. Therefore, the salt stress condition induced for 3 d and 7 d was recognized as the mid-term and long-term stages, respectively.

We observed a consistent increase in the activities of POD, CAT, and increased levels of MDA, proline, Na^+ in leave samples from plants under NaCl-induced salt stress for 3 to 7 d. However, the activity of SOD in leave samples did not change significantly after 3 d of salt stress induction, which was consistent with the previous study on *S.* alopecuroides roots under salt stress conditions [30]. Levels of reactive oxygen species (ROS), including superoxide radicals, hydrogen peroxide (H_2O_2), and hydroxyl radicals (OH^-), increased under salt stress, which was harmful to the normal growth and development of plants [45]. In plants, antioxidant enzymes, including SOD, POD, CAT, glutathione-S-transferases (GST), and glutathione peroxidases (GPX), counters ROS's negative impact [46]. Under salt stress conditions for 3 d, change in POD (1.8 folds) activity was higher than that in CAT and SOD activities. However, after 7 d of salt stress condition, the change in SOD (1.79 fold) activity was higher than the other two enzymes, which indicates that antioxidant enzymes consistently provided defense against salt-induced oxidative damage at different stages of salt stress. The content of MDA increased from 9.31 ± 0.13 to 13.74 ± 0.11 and 9.24 ± 0.04 to 14.54 ± 0.18 in *S. alopecuroides* leaves under NaCl induced salt-stress for 3 d and 7 d. MDA is an important indicator of cell membrane lipid peroxidation and plasma membrane damage [47]. Generally, the higher the MDA content, the higher is the damage to the plasma membrane. The results of this study indicated relatively mild damage to the plasma membrane of *S. alopecuroides,* indicating significant salt tolerance of *S. alopecuroides* under 3 d of salt stress.

Under salt stress, the combination of multiple omics technologies is crucial to elucidate biological processes and identify candidate genes and molecular regulatory mechanisms of different tissues in *S. alopecuroides.*

4.2. Mid-term salt stress (3 d) activated important signaling pathways related to "the secondary messenger"

GO enrichment analysis of DAPs showed that several transporter proteins participated in the mid-term salt stress, and these proteins were related to the secondary messenger signaling pathways, such as phosphatidylinositol signaling system, cAMP signaling pathway, and calcium signaling pathway (Figures 6A and 7A). These proteins primarily included two hexose transmembrane transporters (TRINITY_DN305592_c0_g1; TRINITY_DN298137_c0_g1), one calcium: sodium antiporter (TRINITY_DN295753_c5_g2), one potassium ion transporter (TRINITY_DN293190_c2_g3), two transporters with ATPase activity (TRINITY_DN292809_c0_g3; TRINITY_DN287127_c1_g3), one vacuolar transporter (TRINITY_DN300353_c3_g1), one regulation of vesicle-mediated transporter (TRINITY_DN302691_c1_g1), one oxaloacetate, malate transmembrane transporter (TRINITY_DN299652_c0_g2) (Table S9). Out of these transporter proteins, 16 were up-regulated, and 2 were down-regulated (TRINITY_DN289315_c0_g1; TRINITY_DN300353_c3_g1). The highest fold-change of 1.89 folds (TRINITY_DN292809_c0_g3) and the lowest fold-change of 0.74 times (TRINITY_DN289315_c0_g1) was observed in the F *vs.* Z group.

The most significant adverse effect of salt stress was on the Na^+ and Cl^- accumulation in plant cells and tissues, which resulted in osmotic stress, ion toxicity, and oxidative damage [48–50]. Salt stress has an antagonistic or synergistic effect on certain ions, depending on the experimental design of salt stress and plant tissues and species diversity [51,52]. As per previous reports, salt stress had an antagonistic effect on Ca^{2+}, K^+, Fe, P, and Zn [53–57]. The ion imbalance phenomenon, in

turn, triggers major physiological and biochemistry disorders culminating in plant cell death. Two major processes that help plants adapt to salt stress are enhanced efflux and compartmentalization of Na^+ in vacuoles and accumulation of soluble substances, such as organic solutes, free sugar, glycine betaine, and proline to deal with the change of osmotic pressure [58,59]. Several transporters are involved in Na^+ compartmentalization (TRINITY_DN300353_c3_g1, TRINITY_DN302691_c1_g1) and K^+, Ca^{2+}, Na^+ transportation. This indicates that the transporters identified in the current study might play crucial roles in ionic homeostasis at the mid-term salt stress in the *S. alopecuroides* leaves. Increased salt stress significantly increased the total soluble carbohydrate content of two medicinal plants, *Salvia officinalis,* and *Satureja hortensis* [60,61]. In the current study, protein expression of two hexose transmembrane transporters was up-regulated, which suggested that carbohydrates might be an important compatible compound in *S. alopecuroides*, in line with the findings in rice [62].

It was referred to as quick osmotic signaling and ionic signaling when plants face various adversities [63]. Several chemicals, including Ca^{2+}, cyclic nucleotides, polyphosphoinositides, cyclic AMP (cAMP) , nitric oxide (NO), and sugars, are critical to linking various stress signals and controlling downstream stress responses [64]. The expression level of the gene encoding phosphatidylinositol-specific phospholipase C in *Arabidopsis*, which depends on Ca^{2+}, was increased upon salt stress induction [65]. Phosphatidylinositol 3-kinase could mediate endocytosis under salt stress conditions, leading to ROS synthesis in cells [66]. Although excessive ROS leads to oxidative stress in plants, it positively affects the early signal transduction pathway in response to salt tolerance [66]. It was found that cAMP in plants plays an important role in transcriptional regulation; tolerance to salt stress decreased when the level of cell cAMP increased [67]. We observed that cAMP in plants also plays a crucial role in protein level and regulates tolerance to salt stress. The outcomes of the current study demonstrated that the phosphatidylinositol signaling system, cAMP signaling pathway, and calcium signaling pathway play a crucial role in the mid-term salt stress in the *S. alopecuroides* leave.

4.3. Long-term salt stress (7 d) activated secondary metabolic pathways

GO enrichment analysis of differential proteins demonstrated the involvement of certain transferase, oxidoreductase, and dehydrogenase in the biosynthesis of flavonoids, alkaloids, phenylpropanoids, and metabolism of certain amino acids under long-term salt stress conditions (7 d) (Table S10). These proteins mainly include one flavonol-3-*O*-glucoside L-rhamnosyltransferase (TRINITY_DN296025_c7_g3), one flavonoid 3′-monooxygenase (TRINITY_DN303914_c5_g2), and two acyltransferases (TRINITY_DN296366_c6_g1; TRINITY_DN306231_c2_g1), which participate in flavonoid biosynthesis. One amine oxidase (TRINITY_DN292335_c3_g1), one aldehyde dehydrogenase (TRINITY_DN302217_c2_g1), and two oxidoreductases (TRINITY_DN305695_c1_g1; TRINITY_DN301839_c4_g1) were involved in isoquinoline, pyridine alkaloid biosynthesis, and phenylalanine metabolism. Two identified iron transporters (TRINITY_DN301339_c1_g1; TRINITY_DN289736_c6_g1) were involved in mineral absorption. Out of these proteins that are mainly related to secondary metabolic pathways, 5 were up-regulated, and 6 were down-regulated. The highest fold-change of 1.39 times (TRINITY_DN296366_c6_g1; TRINITY_DN306231_c2_g1) and the lowest fold-change of 0.66 times (TRINITY_DN301339_c1_g1) were observed in the T *vs.* Z group.

Flavonoids are a class of low molecular weight phenolic compounds, including tannins, chalcones, anthocyanins, procyanidins, rutin, and so on [68]. Secondary metabolites widely occur in plants. Out of these secondary, flavonoids have gained a lot of attention from pharmacologists, nutritionists, and botanists due to their antioxidant activity, potential cytotoxicity, free radical scavengers, anti-viral anti-inflammatory, and anti-cancer effects [69–71]. The content and types of flavonoids are related to the plant's tolerance to salt stress. It is especially worth noting that the MYB transcription factor family members in plants play a crucial role in this process [72–74]. For instance, the *Arabidopsis* MYB111 is a positive regulator of salt stress, which functions by binding directly to the cis-acting element in the promoter region of genes encoding flavonoid synthesis enzymes [75].

Transcriptional activity of chalcone synthase (*CHS*), flavanone carboxylase (*F3H*), and flavonol synthase 1 (*FLS1*) increases ROS removal. Tobacco NtMYB4 negatively regulates *NtCHS1* gene expression, reduces flavonoid rutin production, and reduces ROS scavenging under salt stress response [76]. Overexpression of *Arabidopsis* silencing inhibitor (AtROS1) conferred salt stress tolerance to transgenic tobacco, possibly through demethylation, increasing the expression levels of genes encoding flavonoid biosynthesis and antioxidant pathway enzymes [77]. In this study, we observed that certain proteins with flavonoid biosynthesis function were up-regulated under salt stress conditions, indicating activation of some regulatory mechanism in the *S. alopecuroides* leaves in response to salt stress conditions.

Alkaloids are derived from amino acids, such as benzylisoquinoline alkaloids (BIA), which are derived from tyrosine [78]. In plants and some animals, alkaloids are synthesized as secondary metabolites. Currently, > 3000 alkaloids have been identified in more than 4000 different plant species, which participate in a myriad of functions even at low concentrations [79]. Multiple studies have reported that salt-tolerant plants contain higher alkaloid content and antioxidant activity [80]. Some salt tolerance mechanisms are partly due to higher phenylalanine ammonia-lyase (PAL) enzyme activity, which is a key enzyme for phenylpropanoids synthesis [81].

As shown in a previous study, salt treatment increased total alkaloid content in young leaves of *Datura innoxia* Mill [82]. Up-regulation of the gene encoding stylopine synthase resulted in an increased level of the main alkaloid, dihydrocoptisine, in the *Chelidonium majus* leaves under salt stress conditions [83]. The application of secondary chitosan nanoparticles (CSNP) on *Catharanthus roseus* could resist salt stress by enhancing antioxidant activity and alkaloid content [84]. The outcomes of this study showed that it altered the expression of certain secondary metabolism-related enzymes, primarily flavonoids, and alkaloids, to counter the damage to *S. alopecuroides* leaves due to long-term salt stress (7 d). Effects and regulation of salt stress on the expression of these proteins and the content of secondary metabolites remains unclear. In this study, we quantified the matrine and oxymatrine levels, two extensively studied medicinal ingredients in *S. alopecuroides.* The results showed that the matrine and oxymatrine concentrations varied in root, stem, and leaves of *S. alopecuroides*. The highest matrine concentration was observed in the *S. alopecuroides* leaves.

Thus, we concluded that salt stress could reduce sophocarpine and matrine (MA) content in the root, stem, and leaves of *S. alopecuroides* and their relatively higher content was found in leaves. However, the highest oxysophocarpine and oxymatrine (OMA) content was observed in the *S. alopecuroides* stem, which demonstrated that the trend of alkaloid content was different in plant tissues under salt stress conditions (Figure 8).

Different alkaloids have different pharmacological functions, such as anti-cancer, anti-inflammation, anti-fibrosis, anti-virus, and anti-arrhythmia regulations [25]. Therefore, we speculated that different alkaloids participated in different metabolic pathways to cope with salt stress in *S. alopecuroides* L. Besides, protein expression levels of certain enzymes involved in secondary metabolic pathways were altered under salt stress conditions. Similar functional enzymes involved in secondary metabolic pathways were also detected. For example, in our previous study, we observed *lysine decarboxylase* (*LDC*) mRNA expression, which catalyzes the first step in the biosynthetic pathway of quinolizidine alkaloids (QAs). *LDC* was up-regulated in various tissues of *S. alopecuroides* L during seed germination under salt stress conditions [85]. However, altered expression of LDC protein was not observed in the current study. It might be related to experimental treatment conditions, technical methods, and differences in the regulatory pathways of various

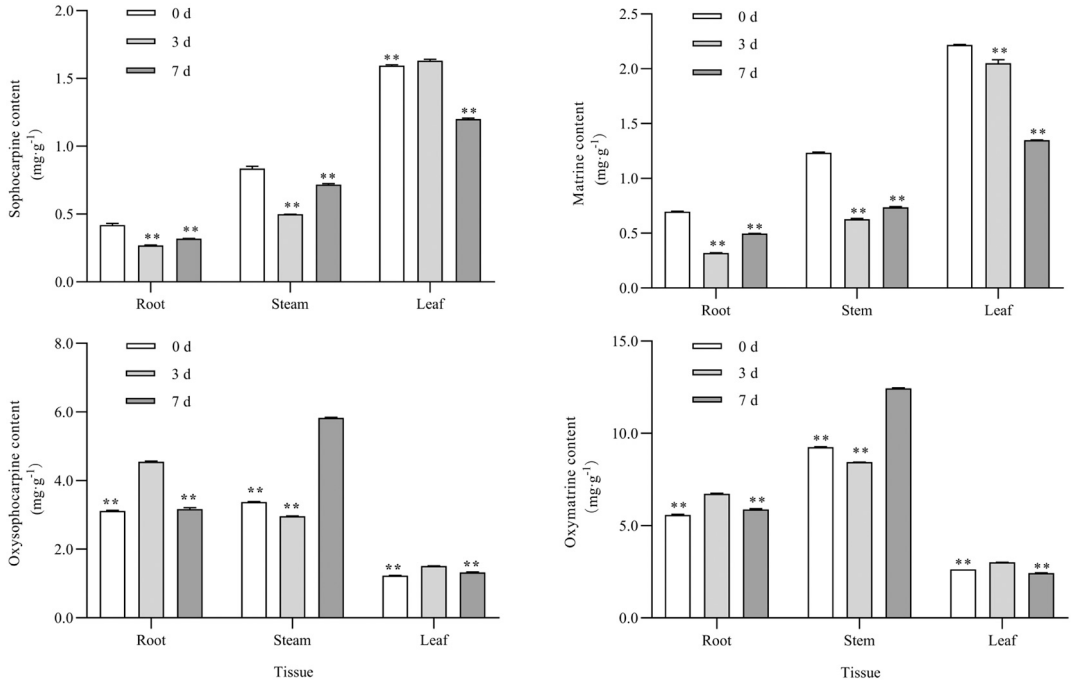

Fig. 8. Determination of sophocarpine, matrine, oxysophocarpine, and oxymatrine contents in different tissues of *S. alopecuroides* seedlings under salt stress.

secondary metabolites under salt stress.

Under salt stress conditions, various secondary metabolites' synthesis and degradation pathways were affected by multiple other factors. The molecular genetic mechanism of *S. alopecuroides* mediated by secondary metabolites in response to salt stress is complex and tissue-specific. As a medicinal plant, *S. alopecuroides* is beneficial for humans because it contains more types and higher content of secondary metabolites. However, balancing the natural growth and development of plants and increasing levels of effective medicinal ingredients demands in-depth investigation. A previous study in Apocyni Veneti Folium reported obtaining higher bioactive components with the dominant type of photosynthetic pigments, osmotic homeostasis, and antioxidant enzyme activity under low salt-stress conditions [86]. The relationship between salt stress and secondary metabolites is highly significant. The differentially expressed genes identified in the current proteomic study could be studied further in future research studies.

4.4. In-depth analysis to identify possible salt tolerance genes

Protein-protein interaction and protein network are pivotal components of the regulatory mechanism for various biological functions. Aggregated proteins in the protein network might have identical functions and may be key proteins influencing metabolism or signal transduction pathways. As described in 4.2 and 4.3, in this study, several transporter proteins involved in the secondary messenger signaling pathways in the mid-term salt stress (3 d) (Table S9) and certain transferase, oxidoreductase, and dehydrogenase in the biosynthesis of flavonoids, alkaloids metabolism under long-term salt stress conditions (7 d) were enriched in the GO functional category (Table S10). These proteins were analyzed thoroughly and systematically. Protein-protein interaction (PPI) analysis on the six clusters of DAPs (Fig. S4) was performed. Expect for the 5th cluster rest of the protein clusters showed protein interaction. According to the criteria for connecting at least two proteins, a total of 23 proteins were selected from all PPI results (Table S11). There were 15 proteins with functional annotations, and 2 of them were consistent with Table S9. We analyzed the significantly enriched pathways, and certain enzymes were found to be involved in phenylalanine metabolism, isoquinoline alkaloid biosynthesis, or tropane, piperidine, and pyridine alkaloid biosynthesis, and other enzymes were involved in flavonoid biosynthesis (Fig. S5). The expression of 12 proteins corresponding to these enzymes was differentially expressed (Table S12), and 5 of them were consistent with the data shown in Table S10. A total of 7 proteins analyzed were identified as possible salt-tolerant genes *via* GO analysis, PPI interaction, and pathway analysis (Table 4).

The protein TRINITY_DN296366_c6_g1 encoding chalcone synthase (EC 2.3.1.74) catalyzes the first committed step in the biosynthesis of flavonoids and participates in the phloretin formation. Generally, chalcone synthase contains many gene family members in plants, and multiple studies have shown that the mRNA level of *CHS* was induced by NaCl [87–89]. The expression of *EaCHS1* and the *AeCHS* in transgenic plant *Eupatorium adenophorum* and *Abelmoschus esculentus*, respectively, regulate flavonoid accumulation and improve resistance to salt stress during seed germination and root development by maintaining ROS homeostasis [90,91]. The protein TRINITY_DN303914_c5_g2 encoding

Table 4
The list of salt tolerance genes in *Sophora alopecuroides*.

Protein	Description	KEGG pathway
TRINITY_DN296366_c6_g1	EC 2.3.1.74, Chalcone synthase EC 2.3.1.170, 6′-deoxychalcone synthase	Flavonoid biosynthesis
TRINITY_DN303914_c5_g2	EC 1.14.14.82, Flavonoid 3′-monooxygenase, CYP75B1 (gene name) or Flavonoid 3′-hydroxylase	
TRINITY_DN306231_c2_g1	EC 2.3.1.133, Shikimate O-hydroxycinnamoyltransferase	
TRINITY_DN301839_c4_g1	EC 1.13.11.27, 4-hydroxyphenylpyruvate dioxygenase	Phenylalanine metabolism
TRINITY_DN292335_c3_g1	EC 1.4.3.21, Primary-amine oxidase	Phenylalanine metabolism Isoquinoline alkaloid biosynthesis
TRINITY_DN299652_c0_g2	Oxaloacetate and/or malate transporter	Gluconeogenesis
TRINITY_DN298137_c0_g1	Carbohydrate and a proton symporter	Glucose transport metabolism

flavanone 3-hydroxylase (EC 1.14.14.82), also known as flavonoid 3′-monooxygenase and CYP75B1), is an important enzyme of the flavonoid pathway. The expression of the *flavanone 3-hydroxylase* gene was found to be increased in salt-tolerant wheat (*Triticum aestivum* L.) cultivar compared to the salt-sensitive wheat cultivar [92]. *Flavanone 3-hydroxylase* gene in tea (*Camellia sinensis*) and Antarctic moss (*Pohlia nutans*), confer tolerance to salt stress [93,94]. The protein TRINITY_DN306231_c2_g1 encoding shikimate O-hydroxycinnamoyltransferase (EC 2.3.1.133) is a certain acyltransferase. The overexpression of *Populus hydroxycinnamoyltransferase* significantly increased the tolerance of transgenic *Arabidopsis* to salt stress due to high ferulate content in lipophilic polyester [95]. The protein TRINITY_DN301839_c4_g1, encoding 4-hydroxyphenylpyruvate dioxygenase (EC 1.13.11.27), is a key enzyme in tyrosine catabolism. It is involved in the biosynthesis of cofactor plastoquinone and tocopherols [96]. Therefore, this enzyme became the molecular target of herbicide design. Transgenetic plants over-expressing bacterial *4-hydroxyphenylpyruvate dioxygenase* were found to be resistant to herbicide [97]. A recent study reported that overexpression of the *4-hydroxyphenylpyruvate dioxygenase* (*IbHPPD*) increased salt tolerance in transgenic sweet potato by inducing enhancement of α-tocopherol and ABA contents [98]. The protein TRINITY_DN292335_c3_g1 encoding primary-amine oxidase (EC 1.4. 3.21, PrAOs, also known as copper-containing amine oxidases, CAOs) catalyzes the oxidation of primary amines into aldehydes. Previous studies have shown that salt stress strongly promoted diamine oxidase activity to stimulate polyamine (PA) degradation in maize seedlings [99]. MA and OMA are the crucial component of *S. alopecuroides*. Lysine decarboxylase (LDC) is the first key enzyme in the biosynthesis of OMA and MA, which catalyzes the decarboxylation of lysine to cadaverine. Our previous results showed that the content of cadaverine in seeds of *S. alopecuroides* was significantly reduced under salt stress conditions [85], which may be related to the increase in CAO enzyme activity. However, a further in-depth study is required to investigate it. The protein TRINITY_DN299652_c0_g2 is involved in the transport of oxaloacetate and malate, which is related to gluconeogenesis. The overexpression of *malate transporter* (*MdALMT14*) in apple calli enhanced salt tolerance by promoting the accumulation of malic acid in apple [100]. The protein TRINITY_DN298137_c0_g1 is a carbohydrate and a proton symporter, which contains multiple gene family members in plants, and is usually involved in the distribution of sugar in the cells. Plants use sugar transporter-mediated sugar compartments as an adaptive strategy against biotic and abiotic stresses [101]. The mutant *atsuc2* or *atsuc4* exhibited hypersensitive phenotypes under salt stress conditions [102]. In this study, we firstly utilized proteomics to identify potential salt-tolerant genes in saline-alkaline and drought-tolerant medicinal plant, *S. alopecuroides,* and understand the underlying molecular mechanism for *S. alopecuroides* salt tolerance. The data from this study laid the foundation for crop genetics and breeding and enhanced the current understanding of the salt tolerance mechanism of the plant kingdom.

Supplementary data to this article can be found online at https://doi.org/10.1016/j.jprot.2021.104457.

Author contributions

Ping Liu designed the research. Wen-Juan Li, Yuan-Shu Hong, and Yu-Mei Zhou performed

the research. Wen-Juan Li and Tian-Li Ma analyzed data. Tian-Li Ma wrote and revised the article. Lei Tian, Xiao-Gang Zhang, and Feng-Lou Liu provided valuable suggestions during the design of the research.

Funding

This study was supported by grants from the National Natural Science Foundation of China (grant no. 81760685) and Key Research and Development Program of Ningxia (grant no. 2019BBF02022).

Declaration of Competing Interest

The authors declare that there are no conflicts of interest.

Data availability

Proteomic data are available via ProteomeXchange with identifier PXD027627. The transcriptomics data were uploaded to the SRA database in NCBI. The BioProject accession number is PRJNA748576.

References

[1] H. Ritchie, M. Roser, Land Use, Our World in Data. https://ourworldindata.org/land-use, 2013 (accessed 26/05/2021).
[2] M. Hasanuzzaman, K. Nahar, M. Fujita, Plant response to salt stress and role of exogenous protectants to mitigate salt-induced damages, in: P. Ahmad, M. M. Azooz, M.N.V. Prasad (Eds.), Ecophysiology and Responses of Plants under Salt Stress, Springer, New York, NY, 2013, pp. 25–87.
[3] FAO, Global Network on Integrated Soil Management for Sustainable use of Salt-Affected Soils, FAO Land and Plant Nutrition Management Service Rome, Italy, 2005.
[4] S.A. Shahid, M. Zaman, L. Heng, Soil salinity: Historical perspectives and a world overview of the problem, in: M. Zaman, S.A. Shahid, L. Heng (Eds.), Guideline for Salinity Assessment, Mitigation and Adaptation Using Nuclear and Related Techniques, Springer, Cham, 2018, pp. 43–53.
[5] M.C. Shannon, C.M. Grieve, Tolerance of vegetable crops to salinity, Sci. Hort. 78 (1998) 5–38, https://doi.org/10.1016/S0304-4238(98)00189-7.
[6] N. Katerji, J.W. Van Hoorn, A. Hamdy, M. Mastrorilli, Salt tolerance classification of crops according to soil salinity and to water stress day index, Agric. Water Manag. 43 (2000) 99–109, https://doi.org/10.1016/S0378-3774(99)00048-7.
[7] G. Ondrasek, Z. Rengel, N. Maurović, N. Kondres, V. Filipović, R. Savić, B. Blagojević, V. Tanaskovik, C.M. Gergichevich, D. Romić, Growth and element uptake by salt-sensitive crops under combined NaCl and Cd stresses, Plants 10 (2021) 1202, https://doi.org/10.3390/plants10061202.
[8] M. Qadir, E. Quillérou, V. Nangia, G. Murtaza, M. Singh, R.J. Thomas, P. Drechsel, A.D. Noble, Economics of salt-induced land degradation and restoration, Nat. Resour. Forum 38 (2014) 282–295, https://doi.org/10.1111/1477-8947.12054.
[9] A. Allbed, L. Kumar, Soil salinity mapping and monitoring in arid and semi-arid regions using remote sensing technology: a review, Adv. Remote Sens. 2 (2013) 41262, https://doi.org/10.4236/ars.2013.24040.
[10] K. Al-aghabary, Z. Zhu, Q. Shi, Influence of silicon supply on chlorophyll content, chlorophyll fluorescence, and antioxidative enzyme activities in tomato plants under salt stress, J. Plant Nutr. 27 (2005) 2101–2115, https://doi.org/10.1081/PLN-200034641.
[11] A. El Moukhtari, C. Cabassa-Hourton, M. Farissi, A. Savouré, How does proline treatment promote salt stress tolerance during crop plant development? Front. Plant Sci. 11 (2020) 1127, https://doi.org/10.3389/fpls.2020.01127.
[12] D.M. Almeida, M.M. Oliveira, N.J. Saibo, Regulation of Na^+ and K^+ homeostasis in plants: towards improved salt stress tolerance in crop plants, Genet. Mol. Biol. 40 (2017) 326–345, https://doi.org/10.1590/1678-4685-GMB-2016-0106.
[13] U. İbrahimova, P. Kumari, S. Yadav, A. Rastogi, M. Antala, Z. Suleymanova, M. Zivcak, M. Tahjib-Ul-Arif, S. Hussain, M. Abdelhamid, S. Hajihashemi, X. Yang, M. Brestic, Progress in understanding salt stress response in plants using biotechnological tools, J. Biotechnol. 329 (2021) 180–191, https://doi.org/10.1016/j.jbiotec.2021.02.007.
[14] D.M. Ha-Tran, T.T.M. Nguyen, S.H. Hung, E. Huang, C.C. Huang, Roles of plant growth-promoting Rhizobacteria (PGPR) in stimulating salinity stress defense in plants: a review, Int. J. Mol. Sci. 22 (2021) 3154, https://doi.org/10.3390/ijms22063154.
[15] F. Zulfiqar, M. Ashraf, Nanoparticles potentially mediate salt stress tolerance in plants, Plant Physiol. Biochem. 160 (2021) 257–268, https://doi.org/10.1016/j.plaphy.2021.01.028.
[16] P.B. Heenan, M.I. Dawson, S.J. Wagstaff, The relationship of *Sophora* sect. *Edwardsia* (Fabaceae) to *Sophora tomentosa*, the type species of the genus *Sophora*, observed from DNA sequence data and morphological characters, Bot. J. Linn. Soc. 146 (2004) 439–446, https://doi.org/10.1111/j.1095-8339.2004.00348.x.
[17] M. Iinuma, M. Ohyama, T. Tanaka, Six flavonostilbenes and a flavanone in roots of *Sophora alopecuroides*, Phytochemistry 38 (1995) 519–525, https://doi.org/10.1016/0031-9422(94)00720-E.
[18] M.I. Choudhary, K. Parvez, A. Ahmed, F. Akhtar, M. Nur-e-Alam, N.M. Hassan, Quinolizidine alkaloids from *Sophora alopecuroides*, J. Nat. Prod. 63 (2000) 190–192, https://doi.org/10.1021/np990351v.
[19] L. Zhao, Z. Deng, W. Yang, Y. Cao, E. Wang, G. Wei, Diverse rhizobia associated with *Sophora alopecuroides* grown in different regions of loess plateau in China, Syst. Appl. Microbiol. 33 (2010) 468–477, https://doi.org/10.1016/j.syapm.2010.08.004.
[20] Z. Zhang, X. Fu, D. Lang, C. Zhang, L. Zhou, Y. Zhao, *Sophora alopecuroides* L. response to salt stress at germination and seedling growth stages, J. Med. Plants Res. 5 (2011) 5423–5427, https://doi.org/10.5897/JMPR.9001145.
[21] I. Nosratti, S. Amiri, A. Bagheri, B.S. Chauhan, Environmental factors affecting seed germination and seedling emergence of foxtail sophora (*Sophora*

alopecuroides), Weed Sci. 66 (2018) 71–77, https://doi.org/10.1017/wsc.2017.35.
[22] F. Yan, Y. Zhu, Y. Zhao, Y. Wang, L. Ji, Q. Wang, Y. Liu, De novo transcriptome sequencing and analysis of salt-, alkali-, and drought-responsive genes in *Sophora alopecuroides*, BMC Genomics 21 (2020) 423, https://doi.org/10.1186/s12864-020-06823-4.
[23] D.D. Wei, D. Cheng, W.B. Liu, T. Liu, Y.H. Zheng, Adequate potassium application enhances salt tolerance of moderate-halophyte *Sophora alopecuroides*, Plant Soil Environ. 61 (2015) 364–370, https://doi.org/10.17221/232/2015-PSE.
[24] J. Wan, R. Wang, H. Bai, Y. Wang, J. Xu, Comparative physiological and metabolomics analysis reveals that single-walled carbon nanohorns and ZnO nanoparticles affect salt tolerance in *Sophora alopecuroides*, Environ. Sci. Nano 7 (2020) 2968–2981, https://doi.org/10.1039/D0EN00582G.
[25] R. Wang, X. Deng, Q. Gao, X. Wu, L. Han, X. Gao, S. Zhao, W. Chen, R. Zhou, Z. Li, C. Bai, *Sophora alopecuroides* L.: an ethnopharmacological, phytochemical, and pharmacological review, J. Ethnopharmacol. 248 (2020), 112172, https://doi.org/10.1016/j.jep.2019.112172.
[26] H. Zhou, J. Li, F. Sun, F. Wang, M. Li, Y. Dong, H. Fan, D. Hu, A review on recent advances in aloperine research: pharmacological activities and underlying biological mechanisms, Front. Pharmacol. 11 (2020), 538137, https://doi.org/10.3389/fphar.2020.538137.
[27] M. Zhang, A. Li, Q. Yang, J. Li, L. Wang, X. Liu, Y. Huang, L. Liu, Beneficial effect of alkaloids from *Sophora alopecuroides* L. on CUMS-induced depression model mice via modulating gut microbiota, Front. Cell. Infect. Microbiol. 11 (2021), 665159, https://doi.org/10.3389/fcimb.2021.665159.
[28] N. Duan, Y. Deng, Y. Liu, Y. Zhang, L.G. Zhang, C.Y. Wang, B.B. Liu, The complete chloroplast genome of *Sophora alopecuroides* (Fabaceae), Mitochondrial DNA B Resour. 4 (2019) 1336–1337, https://doi.org/10.1080/23802359.2019.1596760.
[29] Y. Wang, T. Zhou, D. Li, X. Zhang, W. Yu, J. Cai, G. Wang, Q. Guoo, X. Yang, F. Cao, The genetic diversity and population structure of *Sophora alopecuroides* (Faboideae) as determined by microsatellite markers developed from transcriptome, PLoS One 14 (2019), e0226100, https://doi.org/10.1371/journal.pone.0226100.
[30] Y. Zhu, Q. Wang, Y. Wang, Y. Xu, J. Li, S. Zhao, D. Wang, Z. Ma, F. Yan, Y. Liu, Combined transcriptomic and metabolomic analysis reveals the role of phenylpropanoid biosynthesis pathway in the salt tolerance process of *Sophora alopecuroides*, Int. J. Mol. Sci. 22 (2021) 2399, https://doi.org/10.3390/ijms22052399.
[31] A. Santner, M. Estelle, The ubiquitin-proteasome system regulates plant hormone signaling, Plant J. 61 (2016) 1029–1040, https://doi.org/10.1111/j.1365-313X.2010.04112.x.
[32] N.V. Bykova, C. Rampitsch, Modulating protein function through reversible oxidation: redox-mediated processes in plants revealed through proteomics, Proteomics 13 (2013) 579–596, https://doi.org/10.1002/pmic.201200270.
[33] I. Vaseva, J. Sabotič, J. Šuštar-Vozlič, V. Meglič, M. Kidrič, K. Demirevska, L. Simova-Stoilova, The response of plants to drought stress: The role of dehydrins, chaperones, proteases and protease inhibitors in maintaining cellular protein function, in: D.F. Neves, J.D. Sanz (Eds.), Droughts: New Research, Nova Science Publishers Inc., 2012, pp. 1–45.
[34] J.C. Walker, Structure and function of the receptor-like protein kinases of higher plants, Plant Mol. Biol. 26 (1994) 1599–1609, https://doi.org/10.1007/BF00016492.
[35] J.V. Jorrin Novo, Proteomics and plant biology: contributions to date and a look towards the next decade, Expert Rev. Proteomics 18 (2021) 93–103, https://doi.org/10.1080/14789450.2021.1910028.
[36] K. Kosová, P. Vítámvás, I.T. Prášil, J. Renaut, Plant proteome changes under abiotic stress—contribution of proteomics studies to understanding plant stress response, J. Proteome 74 (2011) 1301–1322, https://doi.org/10.1016/j.jprot.2011.02.006.
[37] H. Zhang, B. Han, T. Wang, S. Chen, H. Li, Y. Zhang, S. Dai, Mechanisms of plant salt response: insights from proteomics, J. Proteome Res. 11 (2012) 49–67, https://doi.org/10.1021/pr200861w.
[38] Y. Liu, S. Lu, K. Liu, S. Wang, L. Huang, L. Guo, Proteomics: a powerful tool to study plant responses to biotic stress, Plant Methods 15 (2019) 135, https://doi.org/10.1186/s13007-019-0515-8.
[39] I. Feussner, A. Polle, What the transcriptome does not tell—proteomics and metabolomics are closer to the plants' patho-phenotype, Curr. Opin. Plant Biol. 26 (2015) 26–31, https://doi.org/10.1016/j.pbi.2015.05.023.
[40] C. Buccitelli, M. Selbach, mRNAs, proteins and the emerging principles of gene expression control, Nat. Rev. Genet. 21 (2020) 630–644, https://doi.org/10.1038/s41576-020-0258-4.
[41] Y. Liu, A. Beyer, R. Aebersold, On the dependency of cellular protein levels on mRNA abundance, Cell 165 (2016) 535–550, https://doi.org/10.1016/j.cell.2016.03.014.
[42] M.G. Grabherr, B.J. Haas, M. Yassour, J.Z. Levin, D.A. Thompson, I. Amit, X. Adiconis, L. Fan, R. Raychowdhury, Q. Zeng, Z. Chen, E. Mauceli, N. Hacohen, A. Gnirke, N. Rhind, F. di Palma, B.W. Birren, C. Nusbaum, Trinity: reconstructing a full-length transcriptome without a genome from RNA-Seq data, Nat. Biotechnol. 29 (2011) 644–652, https://doi.org/10.1038/nbt.1883.
[43] N.Q. Dong, H.X. Lin, Contribution of phenylpropanoid metabolism to plant development and plant–environment interactions, J. Integr. Plant Biol. 63 (2021) 180–209, https://doi.org/10.1111/jipb.13054.
[44] A. Sharma, B. Shahzad, A. Rehman, R. Bhardwaj, M. Landi, B. Zheng, Response of phenylpropanoid pathway and the role of polyphenols in plants under abiotic stress, Molecules 24 (2019) 2452, https://doi.org/10.3390/molecules24132452.
[45] L.J. Quan, B. Zhang, W.W. Shi, H.Y. Li, Hydrogen peroxide in plants: a versatile molecule of the reactive oxygen species network, J. Integr. Plant Biol. 50 (2008) 2–18, https://doi.org/10.1111/j.1744-7909.2007.00599.x.
[46] K. Das, A. Roychoudhury, Reactive oxygen species (ROS) and response of antioxidants as ROS-scavengers during environmental stress in plants, Front. Environ. Sci. 2 (2014) 53, https://doi.org/10.3389/fenvs.2014.00053.
[47] E. Tommasino, S. Griffa, K. Grunberg, A. Ribotta, E. Lopez Colomba, E. Carloni, M. Quiroga, C.M. Luna, Malondialdehyde content as a potential biochemical indicator of tolerant *Cenchrus ciliaris* L. genotypes under heat stress treatment, Grass Forage Sci. 67 (2012) 456–459, https://doi.org/10.1111/j.1365-2494.2012.00851.x.
[48] S. Yadav, M. Irfan, A. Ahmad, S. Hayat, Causes of salinity and plant manifestations to salt stress: a review, J. Environ. Biol. 32 (2011) 667–685.
[49] T.J. Flowers, Improving crop salt tolerance, J. Exp. Bot. 55 (2004) 307–319, https://doi.org/10.1093/jxb/erh003.
[50] A.K. Parida, A.B. Das, Salt tolerance and salinity effects on plants: a review, Ecotoxicol. Environ. Saf. 60 (2005) 324–349, https://doi.org/10.1016/j.ecoenv.2004.06.010.
[51] V.N. Bhivare, J.D. Nimbalkar, Salt stress effects on growth and mineral nutrition of French beans, Plant Soil 80 (1984) 91–98, https://doi.org/10.1007/BF02232942.
[52] G. Villora, D.A. Moreno, G. Pulgar, L. Romero, Yield improvement in zucchini under salt stress: determining micronutrient balance, Sci. Hort. 86 (2000) 175–183, https://doi.org/10.1016/S0304-4238(00)00149-7.
[53] G. Abbas, M. Saqib, J. Akhtar, M.A. Haq, Interactive effects of salinity and iron deficiency on different rice genotypes, J. Plant Nutr. Soil Sci. 178 (2015) 306–311, https://doi.org/10.1002/jpln.201400358.
[54] A.U. Jan, F. Hadi, M.A. Nawaz, K. Rahman, Potassium and zinc increase tolerance to salt stress in wheat (*Triticum aestivum* L.), Plant Physiol. Biochem. 116 (2017) 139–149, https://doi.org/10.1016/j.plaphy.2017.05.008.
[55] M. Wang, Q. Zheng, Q. Shen, S. Guo, The critical role of potassium in plant stress response, Int. J. Mol. Sci. 14 (2013) 7370–7390, https://doi.org/10.3390/ijms14047370.
[56] Inamullah Amanullah, Dry matter partitioning and harvest index differ in rice genotypes with variable rates of phosphorus and zinc nutrition, Rice Sci. 23 (2016) 78–87, https://doi.org/10.1016/j.rsci.2015.09.006.
[57] G. Naheed, M. Shahbaz, A. Latif, E.S. Rha, Alleviation of the adverse effects of salt stress on rice (*Oryza sativa* L.) by phosphorus applied through rooting medium: growth and gas exchange characteristics, Pak. J. Bot. 39 (2007) 729–737.
[58] D.A. Meloni, M.R. Gulotta, C.A. Martínez, M.A. Oliva, The effects of salt stress on growth, nitrate reduction and proline and glycinebetaine accumulation in *Prosopis alba*, Braz. J. Plant Physiol. 16 (2004) 39–46, https://doi.org/10.1590/S1677-04202004000100006.
[59] H. Hajlaoui, N. El Ayeb, J.P. Garrec, M. Denden, Differential effects of salt stress on osmotic adjustment and solutes allocation on the basis of root and leaf tissue senescence of two silage maize (*Zea mays* L.) varieties, Ind. Crop. Prod. 31 (2010) 122–130, https://doi.org/10.1016/j.indcrop.2009.09.007.
[60] S.F. Hendawy, K.A. Khalid, Response of sage (*Salvia officinalis* L.) plants to zinc application under different salinity levels, J. Appl. Sci. Res. 1 (2005) 147–155.
[61] F. Najafi, R.A. Khavari-Nejad, M.S. Ali, The effects of salt stress on certain physiological parameters in summer savory (*Satureja hortensis* L.) plants, J. Stress Physiol. Biochem. 6 (2010) 13–21.
[62] N. Nounjan, P. Theerakulpisut, Effects of exogenous proline and trehalose on physiological responses in rice seedlings during salt-stress and after recovery, Plant Soil Environ. 58 (2012) 309–315, https://doi.org/10.17221/762/2011-PSE.
[63] K. Kumar, M. Kumar, S.R. Kim, H. Ryu, Y.G. Cho, Insights into genomics of salt stress response in rice, Rice 6 (2013) 27, https://doi.org/10.1186/1939-8433-6-27.
[64] N. Tuteja, S.K. Sopory, Chemical signaling under abiotic stress environment in plants, Plant Signal. Behav. 3 (2008) 525–536, https://doi.org/10.4161/psb.3.8.6186.
[65] T. Hirayama, C. Ohto, T. Mizoguchi, K. Shinozaki, A gene encoding a phosphatidylinositol-specific phospholipase C is induced by dehydration and salt stress in *Arabidopsis thaliana*, Proc. Natl. Acad. Sci. U. S. A. 92 (1995) 3903–3907, https://doi.org/10.1073/pnas.92.9.3903.
[66] Y. Leshem, L. Seri, A. Levine, Induction of phosphatidylinositol 3-kinase-mediated endocytosis by salt stress leads to intracellular production of reactive oxygen species and salt tolerance, Plant J. 51 (2007) 185–197, https://doi.org/10.1111/j.1365-313X.2007.03134.x.
[67] R. Xu, Y. Guo, S. Peng, J. Liu, P. Li, W. Jia, J. Zhao, Molecular targets and biological functions of cAMP signaling in Arabidopsis, Biomolecules 11 (2021) 688, https://doi.org/10.3390/biom11050688.
[68] R.E. Koes, F. Quattrocchio, J.N.M. Mol, The flavonoid biosynthetic pathway in plants: function and evolution, BioEssays 16 (1994) 123–132, https://doi.org/10.1002/bies.950160209.
[69] L. Pourcel, J.M. Routaboul, V. Cheynier, L. Lepiniec, I. Debeaujon, Flavonoid oxidation in plants: from biochemical properties to physiological functions, Trends Plant Sci. 12 (2007) 29–36, https://doi.org/10.1016/j.tplants.2006.11.006.
[70] S. Kumar, A.K. Pandey, Chemistry and biological activities of flavonoids: an overview, Sci. World J. 2013 (2013), 162750, https://doi.org/10.1155/2013/162750.
[71] A.N. Panche, A.D. Diwan, S.R. Chandra, Flavonoids: an overview, J. Nutr. Sci. 5 (2016), e47, https://doi.org/10.1017/jns.2016.41.

[72] F. Mehrtens, H. Kranz, P. Bednarek, B. Weisshaar, The Arabidopsis transcription factor MYB12 is a flavonol-specific regulator of phenylpropanoid biosynthesis, Plant Physiol. 138 (2005) 1083–1096, https://doi.org/10.1104/pp.104.058032.
[73] R. Stracke, H. Ishihara, G. Huep, A. Barsch, F. Mehrtens, K. Niehaus, B. Weisshaar, Differential regulation of closely related R2R3-MYB transcription factors controls flavonol accumulation in different parts of the *Arabidopsis thaliana* seedling, Plant J. 50 (2007) 660–677, https://doi.org/10.1111/j.1365-313X.2007.03078.x.
[74] R. Stracke, O. Jahns, M. Keck, T. Tohge, K. Niehaus, A.R. Fernie, B. Weisshaar, Analysis of PRODUCTION OF FLAVONOL GLYCOSIDES-dependent flavonol glycoside accumulation in *Arabidopsis thaliana* plants reveals MYB11-, MYB12- and MYB111-independent flavonol glycoside accumulation, New Phytol. 188 (2010) 985–1000, https://doi.org/10.1111/j.1469-8137.2010.03421.x.
[75] B. Li, R. Fan, S. Guo, P. Wang, X. Zhu, Y. Fan, Y. Chen, K. He, A. Kumar, J. Shi, Y. Wang, L. Li, Z. Hu, C.P. Song, The Arabidopsis MYB transcription factor, MYB111 modulates salt responses by regulating flavonoid biosynthesis, Environ. Exp. Bot. 166 (2019), 103807, https://doi.org/10.1016/j.envexpbot.2019.103807.
[76] S. Chen, F. Wu, Y. Li, Y. Qian, X. Pan, F. Li, Y. Wang, Z. Wu, C. Fu, H. Lin, A. Yang, NtMYB4 and NtCHS1 are critical factors in the regulation of flavonoid biosynthesis and are involved in salinity responsiveness, Front. Plant Sci. 10 (2019) 178, https://doi.org/10.3389/fpls.2019.00178.
[77] P. Bharti, M. Mahajan, A.K. Vishwakarma, J. Bhardwaj, S.K. Yadav, AtROS1 overexpression provides evidence for epigenetic regulation of genes encoding enzymes of flavonoid biosynthesis and antioxidant pathways during salt stress in transgenic tobacco, J. Exp. Bot. 66 (2015) 5959–5969, https://doi.org/10.1093/jxb/erv304.
[78] J.M. Hagel, J.S. Morris, E.J. Lee, I. Desgagné-Penix, C.D. Bross, L. Chang, X. Chen, S.C. Farrow, Y. Zhang, J. Soh, C.W. Sensen, P.J. Facchini, Transcriptome analysis of 20 taxonomically related benzylisoquinoline alkaloid-producing plants, BMC Plant Biol. 15 (2015) 227, https://doi.org/10.1186/s12870-015-0596-0.
[79] J. Kurek, Introductory chapter: Alkaloids-their importance in nature and for human life, in: J. Kurek (Ed.), Alkaloids - their Importance in Nature and Human Life, IntechOpen, United Kingdom, 2019, pp. 1–7.
[80] S. Şirin, B. Aslım, Determination of antioxidant capacity, phenolic acid composition and antiproliferative effect associated with phenylalanine ammonia lyase (PAL) activity in some plants naturally growing under salt stress, Med. Chem. Res. 28 (2019) 229–238, https://doi.org/10.1007/s00044-018-2278-6.
[81] M.T. Ates, A.B. Yildirim, A.U. Turker, Enhancement of alkaloid content (galanthamine and lycorine) and antioxidant activities (enzymatic and non-enzymatic) unders salt stress in summer snowflake (*Leucojum aestivum* L.), S. Afr. J. Bot. 140 (2021), https://doi.org/10.1016/j.sajb.2021.04.016.
[82] J. Brachet, L. Cosson, Changes in the total alkaloid content of *Datura innoxia* mill. Subjected to salt stress, J. Exp. Bot. 37 (1986) 650–656, https://doi.org/10.1093/jxb/37.5.650.
[83] M. Yahyazadeh, R. Meinen, R. Hänsch, S. Abouzeid, D. Selmar, Impact of drought and salt stress on the biosynthesis of alkaloids in *Chelidonium majus* L, Phytochemistry 152 (2018) 204–212, https://doi.org/10.1016/j.phytochem.2018.05.007.
[84] F.A.S. Hassan, E. Ali, A. Gaber, M.I. Fetouh, R. Mazruo, Chitosan nanoparticles effectively combat salinity stress by enhancing antioxidant activity and alkaloid biosynthesis in *Catharanthus roseus* (L.) G. Don, Plant Physiol. Biochem. 162 (2021) 291–300, https://doi.org/10.1016/j.plaphy.2021.03.004.
[85] Y.M. Zhou, Y.S. Hong, W.J. Li, P. Liu, L. Tian, Analysis of physiological characteristics and *lysine decarboxylase* gene expression of *sophora alopecuroides* under salt stress, Southwest China, J. Agric. Sci. 33 (2020) 2755–2759, https://doi.org/10.16213/j.cnki.scjas.2020.12.009. (in Chinese).
[86] C. Chen, H. Liu, C. Wang, Z. Liu, X. Liu, L. Zou, H. Zhao, Y. Yan, J. Shi, S. Chen, Metabolomics characterizes metabolic changes of Apocyni Veneti folium in response to salt stress, Plant Physiol. Biochem. 144 (2019) 187–196, https://doi.org/10.1016/j.plaphy.2019.09.043.
[87] S. Dehghan, M. Sadeghi, A. Pöppel, R. Fischer, R. Lakes-Harlan, H.R. Kavousi, A. Vilcinskas, M. Rahnamaeian, Differential inductions of phenylalanine ammonia-lyase and chalcone synthase during wounding, salicylic acid treatment, and salinity stress in safflower, *Carthamus tinctorius*, Biosci. Rep. 34 (2014), e00114, https://doi.org/10.1042/BSR20140026.
[88] S.B. Abdallah, B. Aung, L. Amyot, I. Lalin, M. Lachâal, N. Karray-Bouraoui, A. Hannoufa, Salt stress (NaCl) affects plant growth and branch pathways of carotenoid and flavonoid biosyntheses in *Solanum nigrum*, Acta Physiol. Plant. 38 (2016) 72, https://doi.org/10.1007/s11738-016-2096-8.
[89] S. Chen, X. Pan, Y. Li, L. Cui, Y. Zhang, Z. Zhang, G. Pan, J. Yang, P. Cao, A. Yang, Identification and characterization of chalcone synthase gene family members in *Nicotiana tabacum*, J. Plant Growth Regul. 36 (2017) 374–384, https://doi.org/10.1007/s00344-016-9646-6.
[90] L. Chen, H. Guo, Y. Li, H. Cheng, Chalcone synthase EaCHS1 from *Eupatorium adenophorum* functions in salt stress tolerance in tobacco, Plant Cell Rep. 34 (2015) 885–894, https://doi.org/10.1007/s00299-015-1751-7.
[91] F. Wang, G. Ren, F. Li, S. Qi, Y. Xu, B. Wang, Y. Yang, Y. Ye, Q. Zhou, X. Chen, A chalcone synthase gene *AeCHS* from *Abelmoschus esculentus* regulates flavonoid accumulation and abiotic stress tolerance in transgenic *Arabidopsis*, Acta Physiol. Plant. 40 (2018) 97, https://doi.org/10.1007/s11738-018-2680-1.
[92] M.T. Dugasa, X. Feng, N.H. Wang, J. Wang, F. Wu, Comparative transcriptome and tolerance mechanism analysis in the two contrasting wheat (*Triticum aestivum* L.) cultivars in response to drought and salinity stresses, Plant Growth Regul. 94 (2021) 101–114, https://doi.org/10.1007/s10725-021-00699-4.
[93] M. Mahajan, S.K. Yadav, Overexpression of a tea *flavanone 3-hydroxylase* gene confers tolerance to salt stress and *Alternaria solani* in transgenic tobacco, Plant Mol. Biol. 85 (2014) 551–573, https://doi.org/10.1007/s11103-014-0203-z.
[94] C. Li, S. Liu, X. Yao, J. Wang, T. Wang, Z. Zhang, P. Zhang, K. Chen, PnF3H, a flavanone 3-hydroxylase from the Antarctic moss *Pohlia nutans*, confers tolerance to salt stress and ABA treatment in transgenic *Arabidopsis*, Plant Growth Regul. 83 (2017) 489–500, https://doi.org/10.1007/s10725-017-0314-z.
[95] A.X. Cheng, J.Y. Gou, X.H. Yu, H. Yang, X. Fang, X.Y. Chen, C.J. Liu, Characterization and ectopic expression of a *populus* hydroxyacid hydroxycinnamoyltransferase, Mol. Plant 6 (2013) 1889–1903, https://doi.org/10.1093/mp/sst085.
[96] R. Beaudegnies, A.J. Edmunds, T.E. Fraser, R.G. Hall, T.R. Hawkes, G. Mitchell, J. Schaetzer, S. Wendeborn, J. Wibley, Herbicidal 4-hydroxyphenylpyruvate dioxygenase inhibitors—a review of the triketone chemistry story from a Syngenta perspective, Bioorg. Med. Chem. 17 (2009) 4134–4152, https://doi.org/10.1016/j.bmc.2009.03.015.
[97] N. Dufourmantel, M. Dubald, M. Matringe, H. Canard, F. Garcon, C. Job, E. Kay, J.P. Wisniewski, J.M. Ferullo, B. Pelissier, A. Sailland, G. Tissot, Generation and characterization of soybean and marker-free tobacco plastid transformants over-expressing a bacterial 4-hydroxyphenylpyruvate dioxygenase which provides strong herbicide tolerance, Plant Biotechnol. J. 5 (2007) 118–133, https://doi.org/10.1111/j.1467-7652.2006.00226.x.
[98] S.E. Kim, X. Bian, C.J. Lee, S.U. Park, Y.H. Lim, B.H. Kim, W.S. Park, M.J. Ahn, C. Y. Ji, Y. Yu, Y. Xie, S.S. Kwak, H.S. Kim, Overexpression of *4-hydroxyphenylpyruvate dioxygenase* (*IbHPPD*) increases abiotic stress tolerance in transgenic sweetpotato plants, Plant Physiol. Biochem. 167 (2021) 420–429, https://doi.org/10.1016/j.plaphy.2021.08.025.
[99] J. Kongkiattikajorn, Effect of salinity stress on degradation of polyamines and amine oxidase activity in maize seedlings, Agric, Nat. Resour. 43 (2009) 28–33.
[100] J. Lu, X. Liu, Q.J. Ma, H. Kang, Y.J. Liu, Y.J. Hao, C.X. You, Molecular cloning and functional characterization of the aluminum-activated malate transporter gene *MdALMT14*, Sci. Hortic. 244 (2019) 208–217, https://doi.org/10.1016/j.scienta.2018.08.045.
[101] K. Yamada, Y. Osakabe, Sugar compartmentation as an environmental stress adaptation strategy in plants, Semin. Cell Dev. Biol. 83 (2018) 106–114, https://doi.org/10.1016/j.semcdb.2017.12.015.
[102] X. Gong, M. Liu, L. Zhang, Y. Ruan, R. Ding, Y. Ji, N. Zhang, S. Zhang, J. Farmer, C. Wang, Arabidopsis *AtSUC2* and *AtSUC4*, encoding sucrose transporters, are required for abiotic stress tolerance in an ABA-dependent pathway, Physiol. Plant. 153 (2015) 119–136, https://doi.org/10.1111/ppl.12225.